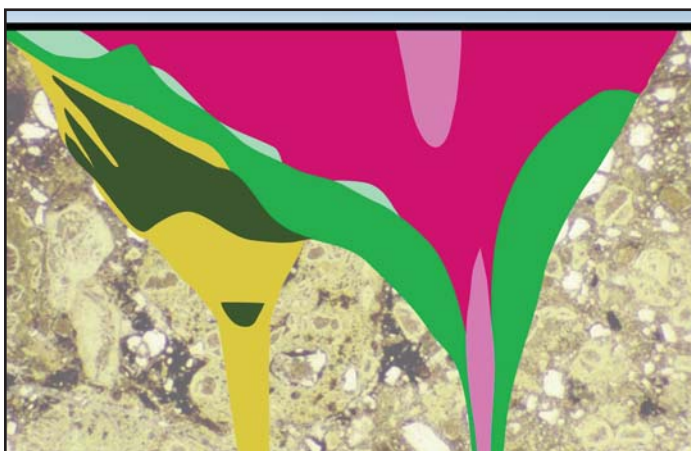# SERIES

Igneous Rock Associations 26. Lamproites, Exotic Potassic Alkaline Rocks: A Review of their Nomenclature, Characterization and Origins

Roger H. Mitchell

Department of Geology, Lakehead University
Thunder Bay, Ontario, P7B 5E1, Canada
Email: rmitchel@lakeheadu.ca

SUMMARY

Lamproite is a rare ultrapotassic alkaline rock of petrological importance as it is considered to be derived from metasomatized lithospheric mantle, and is of economic significance, being the host of major diamond deposits. A review of the nomenclature of lamproite results in the recommendation that members of the lamproite petrological clan be named using mineralogical-genetic classifications to distinguish them from other genetically unrelated potassic alkaline rocks, kimberlite, and diverse lamprophyres. The names "Group 2 kimberlite" and "orangeite" must be abandoned as these rock types are varieties of *bona fide* lamproite restricted to the Kaapvaal craton. Lamproites exhibit extreme diversity in their mineralogy which ranges from olivine phlogopite lamproite, through phlogopite leucite lamproite and potassic titanian richterite-diopside lamproite, to leucite sanidine lamproite. Diamondiferous olivine lamproites are hybrid rocks extensively contaminated by mantle-derived xenocrystic olivine. Currently, lamproites are divided into cratonic (e.g. Leucite Hills, USA; Baifen, China) and orogenic (Mediterranean) varieties (e.g. Murcia-Almeria, Spain; Afyon, Turkey; Xungba, Tibet). Each cratonic and orogenic lamproite province differs significantly in tectonic setting and Sr–Nd–Pb–Hf isotopic compositions. Isotopic compositions indicate derivation from enriched mantle sources, having long-term low Sm/Nd and high Rb/Sr ratios, relative to bulk earth and depleted asthenospheric mantle. All lamproites are considered, on the basis of their geochemistry, to be derived from ancient mineralogically complex K–Ti–Ba–REE-rich veins, or metasomes, in the lithospheric mantle with, or without, subsequent contributions from recent asthenospheric or subducted components at the time of genesis. Lamproite primary magmas are considered to be relatively silica-rich (~ 50–60 wt.% SiO_2), MgO-poor (3–12 wt.%), and ultrapotassic (~ 8–12 wt.% K_2O) as exemplified by hyalo-phlogopite lamproites from the Leucite Hills (Wyoming) or Smoky Butte (Montana). Brief descriptions are given of the most important phreatomagmatic diamondiferous lamproite vents. The tectonic processes which lead to partial melting of metasomes, and/or initiation of magmatism, are described for examples of cratonic and orogenic lamproites. As each lamproite province differs with respect to its mineralogy, geochemical evolution, and tectonic setting there is no simple or common petrogenetic model for their genesis. Each province must be considered as the unique expression of the times and vagaries of ancient mantle metasomatism, coupled with diverse and complex partial melting processes, together with mixing of younger asthenospheric and lithospheric material, and, in the case of many orogenic lamproites, with Paleogene to Recent subducted material.

RÉSUMÉ

La lamproïte est une roche alcaline ultrapotassique rare d'importance pétrologique car elle est considérée comme dérivée du manteau lithosphérique métasomatisé, et d'importance économique, étant l'hôte de gisements de diamants majeurs. Un examen de la nomenclature des lamproïtes conduit à la recommandation que les membres du clan pétrologique des lamproïtes soient nommés en utilisant des classifications minéralogiques génétiques pour les distinguer des autres roches alcalines potassiques génétiquement non liées, de la kimberlite et de divers lamprophyres. Les noms « kimberlite du groupe 2 » et « orangéite » doivent être abandonnés car ces types de roches sont des variétés de véritables lamproïtes

restreintes au craton de Kaapvaal. Les lamproïtes présentent une extrême diversité dans leur minéralogie qui va de la lamproïte à phlogopite et olivine, à la lamproïte à leucite et phlogopite et de la lamproïte à richtérite-diopside potassique titanifère, à la lamproïte à sanidine et leucite. Les lamproïtes à olivine diamantifères sont des roches hybrides largement contaminées par l'olivine xénocristique dérivée du manteau. Actuellement, les lamproïtes sont divisées en variétés cratoniques (par exemple Leucite Hills, États-Unis; Baifen, Chine) et orogéniques (méditerranéennes) (par exemple Murcie-Almeria, Espagne; Afyon, Turquie; Xungba, Tibet). Chaque province de lamproïte cratonique et orogénique diffère significativement par le contexte tectonique et les compositions isotopiques en Sr, Nd, Pb et Hf. Les compositions isotopiques indiquent que leur source est un manteau enrichi, ayant à long terme des rapports Sm/Nd bas et Rb/Sr élevés, par rapport à la Terre globale et au manteau asthénosphérique appauvri. Toutes les lamproïtes sont considérées, sur la base de leur géochimie, comme étant dérivées d'anciennes veines minéralogiquement complexes riches en K, Ti, Ba et ETR, ou métasomes, dans le manteau lithosphérique avec ou sans contributions ultérieures de composants asthénosphériques ou subductés récents au moment de la genèse. Les magmas primaires de lamproïte sont considérés comme relativement riches en silice (~ 50–60% en poids de SiO_2), pauvres en MgO (3–12% en poids) et ultrapotassiques (~ 8–12% en poids de K_2O) comme le montrent les lamproïtes hyalo à phlogopite de Leucite Hills (Wyoming) ou de Smoky Butte (Montana). De brèves descriptions sont données des cheminées de lamproïtes diamantifères phréatomagmatiques les plus importantes. Les processus tectoniques qui conduisent à la fusion partielle des métasomes et / ou à l'initiation du magmatisme sont décrits comme des exemples de lamproïtes cratoniques et orogéniques. Comme chaque province de lamproïte diffère en ce qui concerne sa minéralogie, son évolution géochimique et son cadre tectonique, il n'y a pas de modèle pétrogénétique simple ou commun pour leur genèse. Chaque province doit être considérée comme l'expression unique de l'époque et des caprices du métasomatisme du manteau ancien, associée à des processus de fusion partielle divers et complexes, ainsi qu'à un mélange de matériaux asthénosphériques et lithosphériques plus jeunes et, dans le cas de nombreuses lamproïtes orogéniques, à du matériel paléogène à récent subducté.

Traduit par la Traductrice

INTRODUCTION

Lamproite is a very rare potassic alkaline rock type occurring in less than 50 *bona fide* major petrological provinces on all continents. In this work, a petrological province is regarded as a discrete region of diverse lamproite magmatism of similar age and tectonic setting. Locations of particular lamproite provinces can be found in Mitchell and Bergman (1991), Fareeddudin and Mitchell (2012) or more easily by using Google Earth. Regardless of their rarity they have attained significant importance in the fields of economic geology and mantle petrology. With respect to the former they currently host major diamond mines in Australia (Argyle) and South

Africa (Finsch), with the Argyle AK1 Mine being one of world's highest-grade primary diamond deposits (~30–680 ct/100 t). In terms of mantle petrology, their mineralogy and geochemistry have provided insights into metasomatic processes in the lithospheric mantle which cannot be addressed from investigations of more common magma types.

One objective of this review is to summarize recent revisions to the terminology of the lamproite petrological clan and show how these rock types can be identified correctly using petrography, mineralogy, and isotopic data. The geology of extrusive and hypabyssal lamproite bodies, which is similar to that of common magma types such as basalt, is not described in detail as summaries are given in Jaques et al. (1986), Mitchell and Bergman (1991), and Mitchell (1995a), although aspects of the geology of the most important diamondiferous volcaniclastic and pyroclastic lamproite vents are presented. Although detailed commentary is well beyond the scope of this contribution, the origins of "cratonic" and "orogenic" lamproites, and magma generation in the lithospheric mantle are briefly considered.

The mineralogy of diamonds found in lamproites is not described as, in common with those in kimberlites, these are mantle-derived xenocrysts. Also not considered here are plutonic undersaturated potassic rocks (malignite. pulaskite, missourite, shonkinite, yakutite, synnyrite, etc.) as the relationships of these rocks to lamproite, leucitite, or other potassic magmas have not been resolved. Unfortunately, many of these rocks have been incorrectly termed lamproite. For descriptions of these rock types see Mitchell (1996).

Potassic Alkaline Rocks – Classification

Rocks enriched in K relative to Na are conventionally regarded as potassic alkaline rocks. There is no generally agreed upon definition of the term alkaline, although convention considers alkaline rocks to be those in which the bulk rock alkali (Na and K) content exceeds the alkali feldspar ($NaAlSi_3O_8$ or $KAlSi_3O_8$) molecular ratio of [(Na_2O+K_2O): Al_2O_3:SiO_2] of 1:1:6, with either Al_2O_3 or SiO_2 being deficient (Shand 1922). This definition permits the recognition, with respect to silica (SiO_2), of oversaturated and undersaturated alkaline rocks. Hence, feldspathoidal (nepheline-, leucite-, kalsilite-bearing) rocks are considered to be undersaturated and alkaline, e.g leucitite, kamafugite and nepheline syenite. Silica-rich oversaturated rocks with quartz, containing Na-rich pyroxenes and amphiboles, can also be termed alkaline, e.g. peralkaline granite. Note that the presence of a high content of alkali feldspar or leucite, is usually considered as insufficient grounds for regarding a rock as alkaline. Many rocks containing leucite, such as lamproites, are alkaline by the virtue of being alumina-deficient, regardless of their silica content.

All alkaline rocks can be regarded as belonging to a sodic or potassic series in which the molar K_2O/Na_2O ratio is lesser or greater than unity, respectively. Potassic rocks are further subdivided into potassic rocks with molar K_2O/Na_2O between 1 and 3, and ultrapotassic types with K_2O/Na_2O greater than 3 (Foley et al. 1987). The relative amounts of alkalis to alumina are expressed by the peralkalinity index, i.e. molar

Table 1. *Revised Nomenclature of Lamproites*

Historical name	Revised name
Wyomingite	diopside leucite phlogopite lamproite
Orendite	diopside sanidine phlogopite lamproite
Madupite	diopside madupitic lamproite
Cedricite	diopside leucite lamproite
Mamilite	leucite richterite lamproite
Wolgidite	diopside leucite richterite madupitic lamproite
Fitzroyite	leucite phlogopite lamproite
Verite	hyalo-olivine diopside phlogopite lamproite
Jumillite	olivine diopside richterite madupitic lamproite
Fortunite	hyalo-enstatite phlogopite lamproite
Cancalite	enstatite sanidine phlogopite lamproite

The term *madupitic* is used to reflect the differing *habits and compositions* of phlogopite which have *petrogenetic* significance. Rocks with phenocrystal phlogopite are termed *phlogopite lamproites* and those with poikilitic groundmass phlogopite and tetraferriphlogopite are termed *madupitic lamproites*. This texture might also be termed oikocrystic and the included minerals chadacrysts. Rocks containing both phenocrystal and groundmass mica can be referred to as transitional madupitic lamproite. Note that recently recognized lamproites in Montana, India and Australia are not given type locality names and are described using modal mineralogical criteria *e.g* the Smoky Butte lamproite (Montana) is a hyalo-olivine phlogopite lamproite; the diamond-bearing lamproites at Argyle and Ellendale (W. Australia) and Majhgawan (India) are termed pyroclastic macrocrystal phlogopite olivine lamproites; and the name *orangeite* is now replaced by lamproite *(var. Kaapvaal)* with calcite phlogopite olivine lamproite and diopside sanidine lamproite being common examples.

$[(K_2O+Na_2O)/Al_2O_3]$. If this index is greater than one, a rock is termed peralkaline regardless of the degree of silica saturation.

All lamproites described in this review, are undersaturated potassic or ultrapotassic alkaline rocks with respect to their bulk rock composition. In some instances, such as hyalo-phlogopite lavas, this approximates to parental magma liquid compositions. In contrast, the bulk compositions of alteration-free olivine lamproites, or volcaniclastic lamproites, do not represent liquid compositions because of the high content of mantle- or crustal-derived xenocrysts.

Etymology of Lamproites

The name lamproite was introduced into geological literature by Niggli (1923) and is derived from the Greek root $\lambda\acute{\alpha}\mu\pi\rho\sigma\varsigma$ meaning "glistening", with reference to the common presence of shiny phenocrysts of phlogopite. This term has been retained in the petrological literature regardless that many lamproites do not exhibit this particular characteristic. Currently, lamproites are regarded as a petrological clan of potassic rocks with diverse mineralogical and geochemical characteristics,

which can *only* be recognized using the mineralogical-genetic classification schemes introduced by Scott Smith and Skinner (1984), Mitchell and Bergman (1991) and Woolley et al. (1996).

Unlike common rock types, lamproite and kimberlite cannot be identified by simple optical petrographic studies because of their complex mineralogy and common fine-grained textures. *They cannot be defined using non-genetic International Union of Geological Sciences modal nomenclature schemes* (Mitchell 1995a). Progress in their characterization was only made possible by the development of back-scattered electron petrography coupled with wavelength and energy dispersive X-ray spectrometry. This led to the development of mineralogical-genetic classification schemes for diverse alkaline rocks, and in particular for lamproites and kimberlites (Mitchell and Bergman 1991; Mitchell 1995a; Woolley et al. 1996; Scott Smith et al. 2018). In such schemes, rocks are classified on the basis of typomorphic assemblages of minerals whose compositions are a direct reflection of the composition of their parental magmas. *Identification of all primary minerals is required for correct characterization of a particular sample, including minerals normally considered minor or trace accessory phases.* Note that in mineralogical-genetic classifications it is *not* necessary to know the origins of the parental magmas.

The nomenclature of lamproites has been historically bedevilled by a plethora of type locality names which are unrelated and uninformative. As a result, similarities and relationships between rock types were obscured. This otiose terminology was initially rationalized by Mitchell and Bergman (1991) using a descriptive mineralogical nomenclature scheme (Table 1). *Unlike common rock types it is not possible to devise a simple definition of "lamproite" only on the basis of modal mineralogy, as compositional data for the major, minor, and trace minerals are required for correct identification (see below).* Further, lamproites exhibit an extremely wide range in their modal mineralogy owing to the large number of liquidus phases which can crystallize from compositionally diverse lamproitic magmas.

Rocks which were eventually termed lamproites (Table 1) were initially recognized in the 1890s from the Leucite Hills of Wyoming, USA (wyomingite, orendite, madupite, Cross 1897); subsequently at Almeria and Jumilla in Spain (jumillite, cancalite, verite, fortunite, Osann 1906); and in the 1920s in the West Kimberley region of Australia (cedricite, fitzroyite, mamilite, wolgidite, Wade and Prider 1940). The latter occurrence, was particularly important in that further exploration of this province in the 1970s determined that some lamproites were found to be diamond-bearing, These discoveries led to the development of the AK1 diamond mine in the Argyle pyroclastic lamproite vent as a major source of industrial and rare pink diamonds, and to the recognition of minor deposits of gem quality diamonds in olivine lamproite of the Ellendale area (Jaques et al. 1986). These discoveries prompted reclassification of "anomalous diamond-bearing kimberlites" at Prairie Creek (Arkansas, USA) and Majhgawan (India), as *bona fide* olivine lamproite (Scott Smith and Skinner 1984; Mitchell and Bergman 1991). As a historical note, diamonds were being mined at Majhgawan (formerly Panna) in the early 1800s (Franklin 1822), and this occurrence must now be recognized

as the first known primary diamond deposit in any igneous rock.

Many rocks previously classified as lamproite (*sensu lato*) are actually leucitite and related rock types (Lustrino et al. 2016, 2019), and many "kimberlites and minettes" in the Dharwar, Baster, and Singhbhum cratons of India are now reclassified as lamproite (Mitchell and Fareeduddin 2009; Fareeduddin and Mitchell 2012; Gurmeet Kaur and Mitchell 2013; Shaikh et al. 2019). Note that recently recognized lamproites are not given type locality names (e.g. Moon Canyonite, Vattikodite) and are described using mineralogical-genetic nomenclature, e.g. the Smoky Butte lamproite (Montana) is a hyalo-olivine phlogopite lamproite, and some of the Argyle diamond-bearing lamproites are xenocrystic-quartz-bearing macrocrystic phlogopite olivine lamproite tuff.

Lamproite terminological confusion has been further exacerbated by the formerly received concept that diamonds could only be found in kimberlite. Thus, the two distinct varieties of diamond-bearing rocks found in Southern Africa were initially termed "basaltic" and "micaceous kimberlites" (Wagner 1914). Although the term basaltic was eventually discarded as these rocks are totally unrelated to basalt, the micaceous variety continued to be referred to as kimberlite by Mitchell (1986). The terms Group 1 and Group 2 kimberlite were introduced by Smith (1983) and Smith et al. (1985) to distinguish between kimberlite and micaceous kimberlite primarily on their Sr–Nd isotopic signatures. Subsequently, these terms were unfortunately entrenched in petrological literature in the now otiose IUGS classification scheme of Woolley et al. (1996). However, it is now accepted that Group 1 and 2 kimberlites belong to genetically distinct parental magma types and form separate petrological clans (Dawson 1987; Mitchell 1995a; Scott Smith et al. 2018; Pearson et al. 2019). Thus, use of the term Group 1 kimberlite must be discontinued and these rocks simply referred to as *kimberlite*. Mitchell (1995a) demonstrated that Group 2 or micaceous kimberlites have close mineralogical affinities with lamproites and resurrected an older name "orangeite", as originally recommended by Wagner (1928), who recognized the mineralogical distinctiveness of these rocks. Subsequently, Mitchell (2006, 2007), Scott Smith et al. (2018) and Pearson et al. (2019) have further revised this nomenclature and considered that the southern African micaceous kimberlites are *bona fide* lamproites and represent a suite of rocks derived from ancient metasomatized lithospheric mantle. Thus, the recommended group name for orangeites is now *lamproite variety Kaapvaal*. This term is preferred as it emphasizes the common petrogenesis with lamproites *sensu lato* and eliminates any petrological confusion with petrogenetically distinct kimberlites. To avoid any further confusion and false genetic hypotheses, the term "Group 2 kimberlite" must be abandoned as these rocks are *not* kimberlites.

Although relatively rare rock types, *bona fide* lamproites, have now been recognized from all continents and occur in two distinct tectonic environments, and are currently referred to as cratonic (or anorogenic) lamproites and orogenic lamproites. The latter, also termed Mediterranean lamproites, occur primarily in a belt extending from Spain and Italy through Serbia and Turkey to Tibet. These occurrences are associated with recent subducted plate margins and diverse varieties of subduction-related potassic magmatism.

An occurrence of lamproite-like rocks associated with shoshonite has been described from Lesbos (Aegean Sea) by Pe-Piper et al. (2014), These rocks do not have the typical mineralogy of *bona fide* lamproites, especially with respect to mica composition and paragenesis, with some examples even containing plagioclase. Although isotopic data indicate derivation from light REE-enriched lithospheric mantle, this is considered to have occurred in Paleozoic times. Thus, in contrast to other peri-Mediterranean lamproites these Miocene rocks are not associated with contemporary subduction. The association with shoshonite suggests that these para-lamproites are a unique suite of rocks related to the back-arc extension of island arc volcanism as suggested by Pe-Piper et al. (2014). Mitchell and Bergman (1991) have noted that para-lamproites associated with shoshonite have much in common with island arc boninite (Crawford et al. 1989) for which a low Nd isotopic ratio has been interpreted to indicate derivation from old light REE-enriched mantle (Hickey and Frey 1982). Thus, it is considered that the Lesbos rocks are not *bona fide* lamproites.

Only cratonic varieties of lamproite have been found to be diamondiferous. The most important advance resulting from the reclassification of Group 2 kimberlites and orangeites as lamproites is the renewed emphasis on the diamondiferous character of the Kaapvaal craton lamproites. This has resulted in significant changes in the exploration philosophy used to locate these rocks, as they cannot be identified by methods used to recognize *bona fide* kimberlites, such as the use of magnesian ilmenite as an indicator mineral. Major (Finsch, Lace) and minor (Star, Roberts Victor, Bellsbank) diamond mines are now regarded as lamproite volcanic vents and dykes (a.k.a. fissure mines).

The cratonic varieties of lamproite are the easiest to identify, using the mineralogical and geochemical criteria (see below) developed by Mitchell and Bergman (1991). However, even these rocks exhibit extremely wide variations in their modal mineralogy, and it has been shown that each cratonic lamproite province has a distinct mineralogical, geochemical, and isotopic signature. This is a result of derivation of the parental magmas from modally diverse, but mineralogically similar, metasomatized lithospheric mantle source rocks with high Rb/Sr ratios and low Sm/Nd ratios. Mitchell (2006, 2007) and Scott Smith et al. (2018) have referred to cratonic lamproites as *metasomatized mantle magmas*, which can be given varietal names which reflect their underlying ancient metasomatized cratonic sources, e.g. lamproite (var. Kaapvaal), lamproite (var. Dharwar), lamproite (var. Bundelkhand). In contrast to the Mediterranean lamproites which are associated with recent subduction, cratonic lamproites, on the basis of their Sr–Nd isotope geochemistry, are now known to be derived from source regions containing a geochemical contribution from ancient subduction events (see below).

The orogenic lamproites (e.g. Cancarix, Jumilla, Orciatico, Afyon, Xungba, etc.) present significant challenges to recognition as these are found in geographic and geotectonic settings

(e.g. the Roman Volcanic Province of Italy) in association with leucitite, shoshonite, and other potassic rocks (kamafugite, tephrite, leucite phonolite) whose origins are commonly considered to be related to recent complex subduction processes. These lamproites exhibit many of the same geochemical and mineralogical features as cratonic lamproites, but their genesis is considered to have a greater contribution of recent subducted island arc or oceanic lithospheric components (Conticelli and Manetti 1995; Miller et al. 1999; Conticelli et al. 2002; Prelević and Foley 2007; Gaeta et al. 2011; Lustrino et al. 2016, 2019) compared to the ancient metasomatized mantle sources of cratonic lamproites.

Mineralogical Criteria for Lamproite Recognition

Lamproites exhibit an extraordinarily wide range in texture and modal mineralogy owing to the diverse mineralogy of their mantle sources, whether they are extrusive or intrusive, and/or the products of magmatic differentiation. Many examples of this petrographic diversity are presented in Mitchell (1997). Accordingly, it is usually necessary to examine a suite of rocks in a potential lamproite field rather than basing identification on a single specimen.

Mitchell and Bergman (1991), Mitchell (1995a) and Woolley et al. (1996) considered that typical *cratonic* lamproites might contain the following major primary minerals: titanian (2–10 wt.% TiO_2), Al_2O_3-poor (5–12 wt.%) phlogopite phenocrysts (Fig. 1); titanian (5–10 wt.% TiO_2) groundmass poikilitic tetra-ferriphlogopite (Fig. 2); titanian (3–5 wt.% TiO_2) potassium (4–6 wt.% K_2O) richterite (Fig. 3); euhedral, hopper and/or "dog's tooth" forsteritic olivine (see below) phenocrysts and macrocrysts; Al_2O_3-poor (< 1 wt.%) diopside (Fig. 4); non-stoichiometric Fe-rich leucite (1–4 wt.% Fe_2O_3) (Fig.4); and Fe-rich sanidine (1–5 wt.% Fe_2O_3; Fig.4). Minor and common typomorphic accessory minerals include: priderite [(K₂(Fe²⁺,Mg)Ti₇O₁₆–Ba(Fe³⁺,Cr,Mg)Ti₇O₁₆; wadeite (K₂ZrSi₃O₉); Sr-rich apatite; Sr-rich perovskite; titanian magnesiochromite; armalcolite [(Mg,Fe²⁺)Ti₂O₅]; noonkanbahite–shcherbakovite [(K,Na,Ba)₃(Ti,Nb)₂(Si₄O₁₂]; baotite (Ba₄Ti₈Si₄O₂₈Cl–Ba₄Ti₂Fe²⁺₂Nb₄Si₄O₂₈Cl); ilmenite; and jeppeite [(K,Ba)₂(Ti,Fe³⁺)₆O₁₃]; and other less common K–Ba–V-titanates (haggertyite, mannardite, redledgeite, unnamed K₂Ti₁₂O₂₅).

Kaapvaal lamproites are unusual in that many olivine lamproites (Sover, Bellsbank, Newlands, Swartruggens) contain significant amounts of calcite or dolomite. Pearson et al. (2019) have suggested that these rocks might be termed "carbonate-rich olivine lamproite" rather than "unevolved orangeites" (Mitchell 1995a) to distinguish them from rocks that exhibit typical phlogopite lamproite characteristics (Lace, Voerspoed,, Besterskraal). However, following lamproite mineralogical genetic classifications, "calcite phlogopite olivine lamproite" and "dolomite olivine lamproite" are preferred names. Other carbonate minerals identified in lamproites
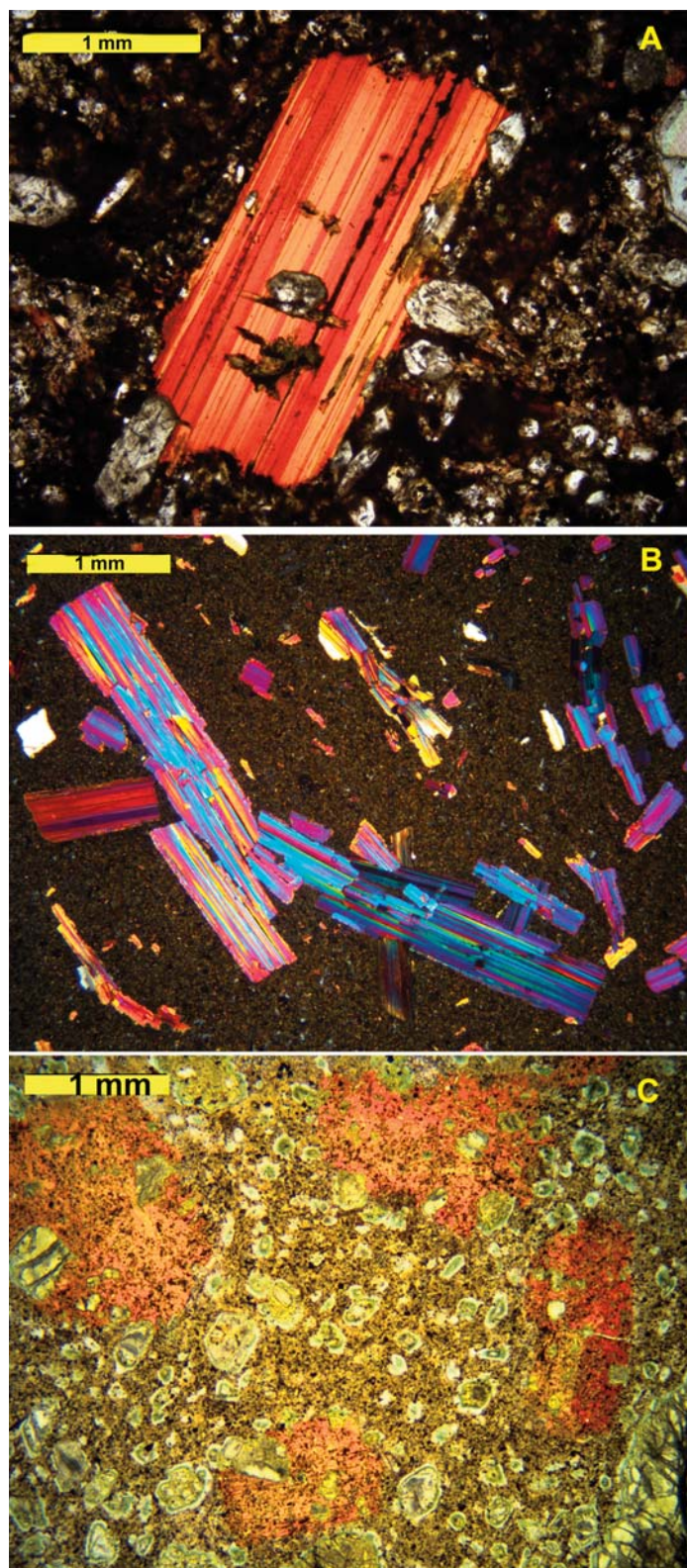

Figure 1. *(above right)* Typical appearance of titanian phlogopite in lamproites. (A) Polysynthetic twining in a phlogopite phenocryst from Mt. North (Ellendale Province) showing the characteristic lemon-yellow to orange-red pleochroism of parallel twins in different optical orientations. (B) Characteristic appearance under crossed polars of polysynthetically twinned titanian phlogopite phenocrysts from 81 Mile Vent (Ellendale Province). (C) Madupitic olivine lamproite from Prairie Creek (Arkansas) showing groundmass poikilitic (or oikocrystic) orange-red pleochroic titanian phlogopite with chadacrysts of diopside, spinel, and perovskite. Subhedral microphenocrysts are serpentinized olivine set in a groundmass of pale-yellow altered glass with spinel, diopside and perovskite.
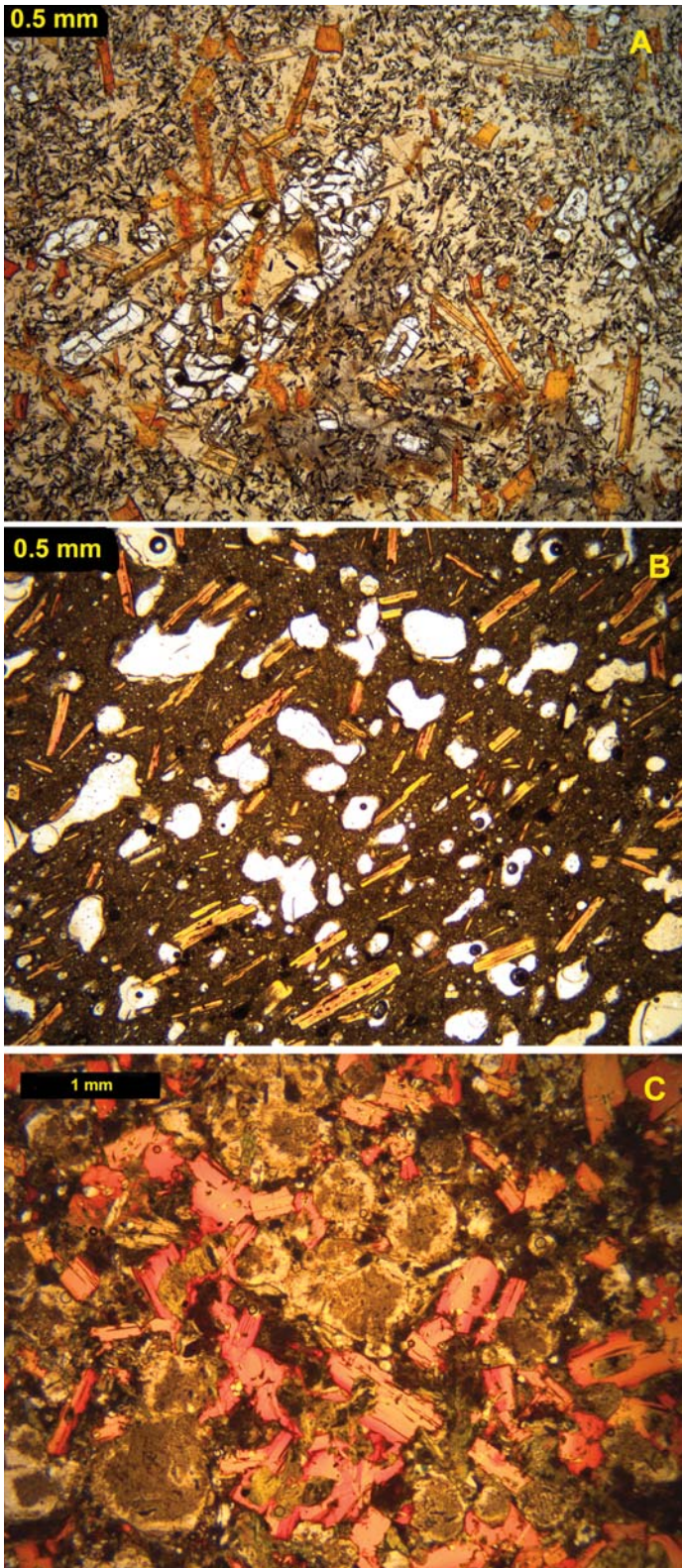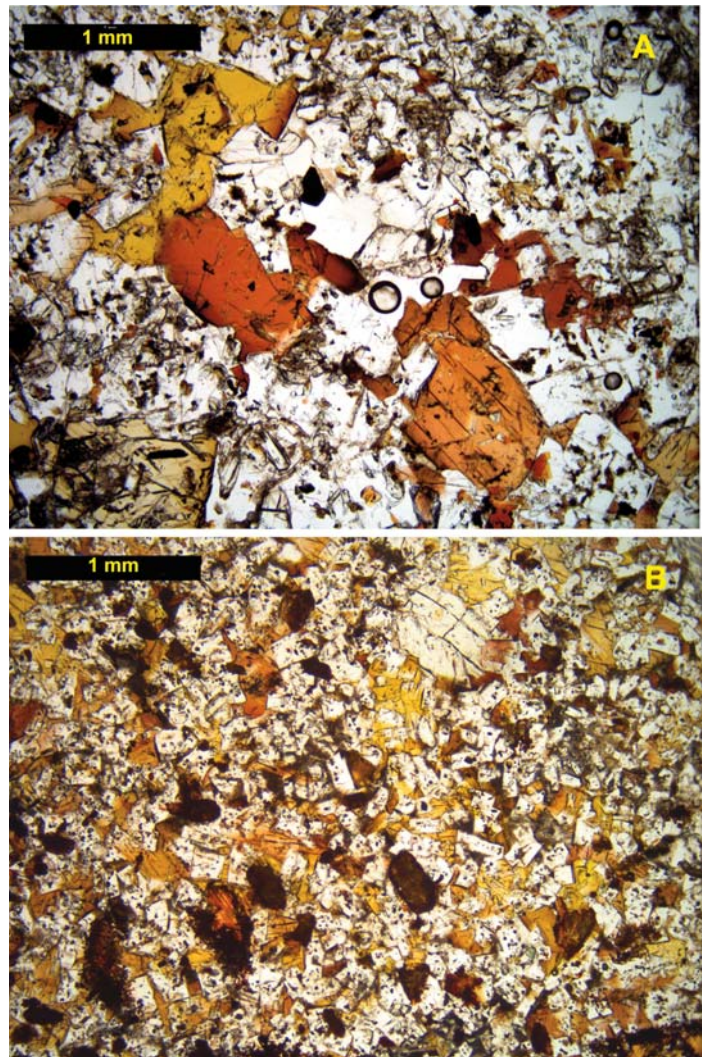
Figure 3. Examples of sanidine amphibole lamproite showing the characteristic lemon-orange to orange-brown pleochroism of groundmass poikilitic K–Ti-richterite. (A) Cancarix Sill (Murcia-Almeria Province) with colourless co-crystallizing potassium feldspar. (B) Moon Canyon (Utah) with microphenocrystal sanidine set in a matrix of K–Ti-richterite.

include witherite, ancylite, barian strontianite and norsethite. Further studies of the carbonate minerals are required.

The compositional trend of evolution from titanian phlogopite to Al-poor tetraferriphlogopite is a hallmark of lamproites and permits their discrimination from superficially similar kimberlites and minettes whose micas evolve to kinoshitalite or aluminous biotite, respectively (Mitchell and Bergman 1991).

Note that the presence of all of the above minerals in a rock is not required in order for it to be classified as a lamproite. Any one mineral might be dominant and in association with others determine the petrographic name.
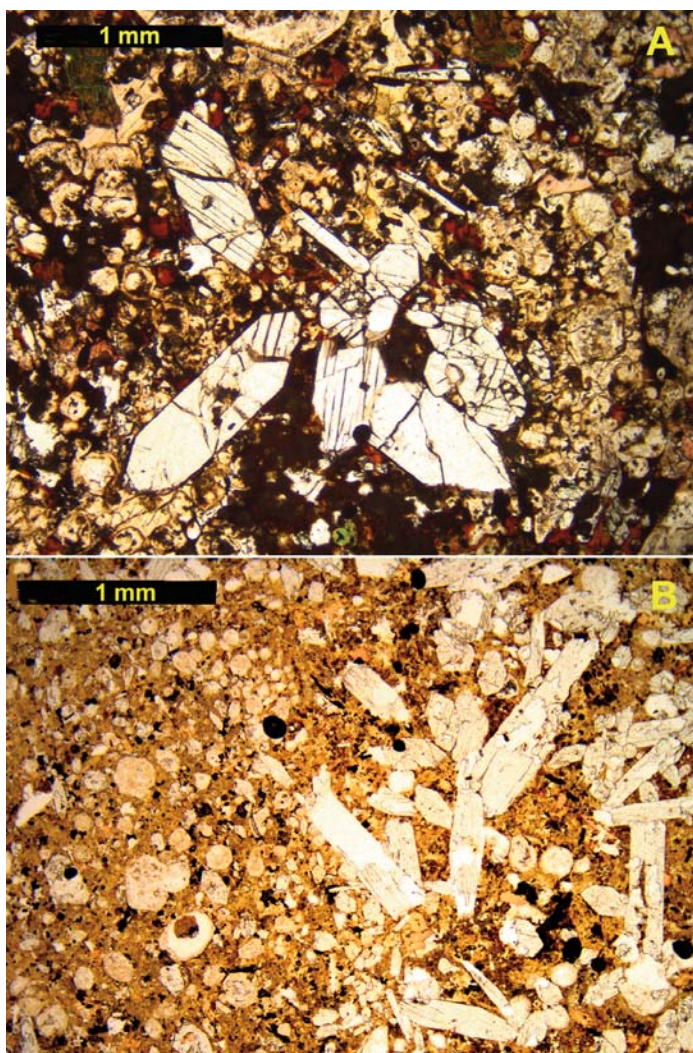
Figure 2. *(above left)* Examples of phlogopite lamproite. (A) Hypabyssal hyalo-phlogopite lamproite from Smoky Butte (Montana) with resorbed phenocrysts of colourless olivine and prismatic phenocrysts of orange titanian phlogopite set in a matrix of microlitic diopside, armalcolite and pale-yellow glass. (B) Vesicular phlogopite lamproite lavas from Zirkel Mesa (Leucite Hills) with yellow-orange titanian phlogopite phenocrysts set in an optically unresolvable matrix containing diopside, altered leucite and glass. (C) Hypabyssal leucite phlogopite lamproite from Raniganj (Damodar Province) showing phenocrysts zoned from orange-yellow cores to red margins of titanian phlogopite. Former leucite is present as icosahedral phenocrysts altered to zeolite.

Figure 4. Examples of diopside leucite lamproite from P Hill (A) and Mt. Gytha (B), (Ellendale Province, West Kimberley) illustrating euhedral colourless diopside phenocrysts set in a matrix of altered microphenocrystal leucite with groundmass titanian phlogopite, K–Ti-richterite.

Orogenic lamproites are less easily recognized although they contain most of the major minerals listed above. In contrast to cratonic types the compositions of amphiboles tend to be more sodic, and potassium feldspars have higher Na_2O (2–3 wt.%) and Ca contents, but the latter rarely exceed 1 wt.% CaO. Typically, but not entirely, orogenic lamproites lack K–Ba-titanates, wadeite and other Ba–Ti-silicate minerals as a consequence of the relative depletion of the parental magmas in Ti, Ba, and Nb. However, many contain ilmenite and/or Ti–Cr-magnetite. Well-differentiated examples from Montecatini contain zircon, quartz, and perrierite (Conticelli et al. 1992), and at Cancarix lamproites contain dalyite, Cr–Zr-armalcolite, britholite, and roedderite (Contini et al. 1993). Further mineralogical studies are required to characterize the accessory mineralogy of orogenic lamproites. These assemblages will probably be quite variable as they depend upon the character and amount of the recent subducted material involved in their genesis.

GEOCHEMICAL CRITERIA FOR LAMPROITE RECOGNITION

Major and Trace Elements
Given the mineralogical heterogeneity of lamproites, it is not particularly useful to formulate geochemical criteria for their recognition. The bulk compositions of most lamproites, apart from glassy or fine-grained vesicular lavas, such as found in the Leucite Hills and at Smoky Butte (Table 2; compositions 1 and 2), do not represent liquid compositions. In addition, most olivine lamproites, in common with kimberlites, contain significant amounts of contamination by mantle-derived olivine xenocrysts and micro-xenoliths (Fig. 5) resulting in high Mg contents (Table 2; compositions 3–7). It is this feature, plus the presence of diamond, which has resulted in the past incorrect classification of many olivine lamproites as kimberlite. Regardless, the undersaturated, potassic nature of the magmas from which lamproite rocks crystallize confers upon their mineralogy some common geochemical characteristics. Thus, following the whole rock geochemical classification schemes of Foley et al. (1987) and Mitchell and Bergman (1991), *cratonic lamproites* are ultrapotassic (molar K_2O/Na_2O >3), commonly peralkaline [molar $(K_2O + Na_2O)/Al_2O_3$ >1] with [$Mg/(Mg + Fe^{2+})$ > 70], with low CaO (< 10 wt.%), high Ba (2000–5000 ppm), Zr (> 500 ppm) and Sr (1000–4000 ppm) contents coupled with high TiO_2 (1–7 wt.%). Note that bulk compositions are a direct reflection of mineralogy and vary within and between lamproite provinces, e.g. 3607–22102 ppm Ba versus 6600–16534 ppm Ba for West Kimberley and Smoky Butte phlogopite lamproites, respectively (Mitchell and Bergman 1991).

Orogenic lamproites are also ultrapotassic as defined by Foley et al. (1987). Compared to cratonic types they are also rich in SiO_2 (~ 48–60 wt.%) and K_2O (3–11 wt.%), and are characterized by relatively low TiO_2 (< 3 wt.%), Al_2O_3 (8–14 wt.%), and CaO (3–4 wt. %) with 0.5–4 wt.% Na_2O (Prelević et al. 2008a). In common with cratonic types they are enriched in LREE, but in contrast are also enriched in Pb (55–150 ppm) relative to cratonic lamproite (e.g. phlogopite lamproite from the Leucite Hills and Smoky Butte, 24–32 ppm and 0.2–44 ppm, respectively). These lamproites are not as enriched in Ba and Zr (< 3000 ppm) as cratonic lamproites, e.g. 1200–3055 ppm Ba and 295–1045 ppm Zr, versus 3065–24800 ppm Ba and 1250–8139 ppm Zr, for Murcia-Almeria and Leucite Hills phlogopite lamproites, respectively. Krmíček et al. (2011) have suggested that a ternary Th–Hf–Nb/2 geochemical discrimination diagram can be used to distinguish cratonic (> 100 ppm Nb) from orogenic lamproites (< 100 ppm Nb). However, in general, trace element discrimination diagrams are not especially useful for lamproite identification as in many instances there is considerable overlap with the compositions of minettes and diverse potassic rocks (Mitchell and Bergman 1991). Prelević et al. (2008b) have concluded from a study of a Turkish lamproite province, in which both cratonic and orogenic lamproites apparently coexist, that the geodynamic distinction of lamproites based only on geochemistry is questionable.

Similar reservations exist with respect to bulk rock incompatible trace element data normalized to primitive mantle com-

Table 2. Representative compositions (wt.%) of cratonic and orogenic lamproites.

	1	2	3	4	5	6	7	8	9	10
SiO_2	55.12	52.94	43.56	39.46	44.10	35.3	28.4	57.2	56.72	60.62
TiO_2	2.58	5.14	2.31	2.61	3.20	1.09	1.24	1.78	1.58	0.86
Al_2O_3	10.35	8.55	7.85	3.53	3.50	2.73	2.94	8.98	13.40	12.88
Fe_2O_3	3.27	5.65	5.57	8.78	4.50			5.89	3.34	5.51
FeO	0.62		0.85		3.09	8.56	7.60		2.42	
MnO	0.06	0.07	0.15	0.13	0.12	0.18	0.33	0.06	0.07	0.10
MgO	6.41	8.38	11.03	26.67	21.30	26.9	15.3	7.99	5.13	5.06
CaO	3.45	4.51	11.89	5.14	3.74	8.43	19.4	3.66	5.27	3.93
SrO	0.26	0.38	0.40	0.14	0.11	0.21	0.19	0.09	0.14	0.10
BaO	0.52	0.86	0.66	0.23	1.05	0.51	0.37	0.22	0.28	0.26
Na_2O	1.29	0.96	0.74	0.29	0.93	0.13	0.15	1.22	2.08	2.62
K_2O	11.77	8.84	7.19	2.56	6.51	2.73	2.66	8.72	8.02	6.23
P_2O_5	1.40	2.21	1.50	0.29	1.13	0.64	1.68	0.83	0.67	0.60
H_2O^+	1.23		2.89	7.70	3.09	5.79	6.98			
CO_2	0.20			0.21	0.28	4.64	9.46		0.02	
LOI		0.83		1.75	2.54				0.01	1.37
Total	99.06	99.32	98.68	99.49	99.19	97.84	96.7	100.09	99.15	100.14

Cratonic lamproites: 1, hyalo-phlogopite lamproite, Steamboat Mountain, Leucite Hills (Carmichael 1967); 2, hyalo-armalcolite phlogopite lamproite, Smoky Butte (Mitchell et al. 1987); 3, madupitic lamproite, Pilot Butte, Leucite Hills (Carmichael 1967); 4, olivine madupitic lamproite, Prairie Creek (Scott Smith and Skinner 1984); 5, olivine lamproite, Ellendale 9, West Kimberley (Jaques et al. 1986); 6, 7, olivine phlogopite lamproites, East Star and Wynandsfontein, respectively, South Africa (Coe et al. 2008).
Orogenic lamproites: 8, phlogopite lamproite, Cancarix, Spain (Venturelli et al. 1984); 9, phlogopite lamproite, Mibale, Tibet (Gao et al. 2007); 10, phlogopite lamproite, Xungba, Tibet (Miller et al. 1999).

positions (a.k.a. spidergrams) as these diagrams were initially devised for whole rock compositions which approximate to melt compositions (i.e basalt) derived from mineralogically simple mantle sources (e.g. garnet lherzolite). *Hence, these diagrams cannot be applied usefully for petrogenetic purposes to magmas derived from heterogeneous multi-phase metasomatized mantle sources.* Attempts to force particular lamproites, e.g. Majhgawan, into pre-existing petrological groups such as kimberlites and "orangeites" are doomed to failure as their mantle sources are different. Hence, there can be no "transitional" magma types and the proposed re-introduction of type locality names, such as "majhgawanite" (Chalapathi Rao 2005), is regressive and petrogenetically unsound. However, these diagrams can be useful for illustrating the significant differences in lamproite geochemistry within and between provinces. Thus, Prelević et al. (2008a, b) have demonstrated that orogenic lamproites exhibit negative anomalies for Rb, Ba, Nb, Ti, Sr, and P with a significant positive Pb anomaly relative to cratonic lamproites (Fig. 6). However, interpretation of these differences requires a thorough knowledge of the tectonic regimes of emplacement.

Isotopic Variations
Isotopic studies have resulted in a better understanding of the mantle origins of lamproites and highlighted the significant differences between cratonic and orogenic types. Current petrogenetic models for lamproites rely extensively on these data. In these models it is considered that the Nd, Sr, Hf, and Pb isotopic compositions (McCulloch et al.1983; Vollmer et al.

1984; Nelson et al. 1986; Mitchell and Bergman 1991; Mitchell 1995a) of cratonic lamproites do not reflect upper crustal contamination and indicate derivation of parental magmas by single stage partial melting of lithospheric mantle sources which have undergone long term enrichment in light REE (i.e. low Sm/Nd ratios) and Rb (i.e. high Rb/Sr ratios), coupled with depletion in U. Each cratonic lamproite province has wide and distinct isotopic compositions reflecting the age and local modal mineralogy, and thus geochemistry, of their metasomatized lithospheric mantle sources. Of particular significance, is that all cratonic lamproites plot on Nd–Sr isotopic diagrams below the bulk Earth Nd composition with Sr isotopic compositions, suggesting extremely wide variations in the apparent Rb/Sr ratios of their sources (Fig. 7). The West Kimberley leucite lamproites are notable in being extremely rich in radiogenic Sr; a feature considered to reflect the high Rb/Sr ratio of their source relative to that of the Smoky Butte lamproites derived from sources with much lower Rb/Sr and very low Sm/Nd ratios (Fig. 7). Note that lamproites differ significantly with respect to kimberlites which have relatively uniform isotopic compositions (Fig.7) and are enriched in radiogenic Nd relative to bulk Earth and depleted in radiogenic Sr, suggesting derivation from REE-depleted asthenospheric sources (Pearson et al. 2019) with ancient low Rb/Sr and high Sm/Nd ratios.

Orogenic lamproites also exhibit an extremely wide range in Sr, Nd, Pb, and Hf isotopic compositions with notable differences between eastern (Serbia, North Macedonia, Turkey) and western provinces (Spain, Italy), and Tibet (Fig. 7; Miller et
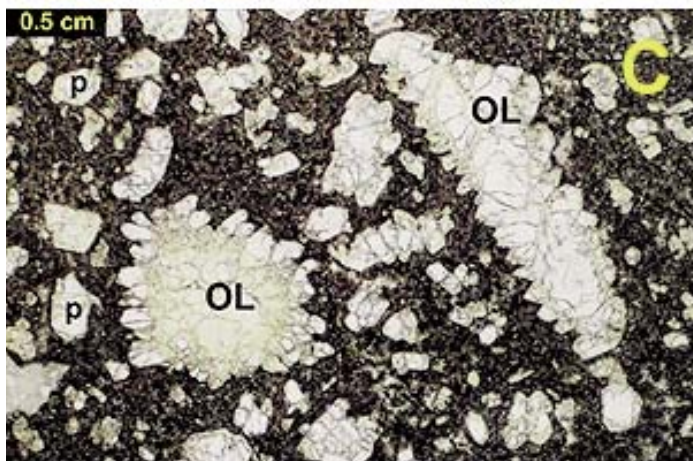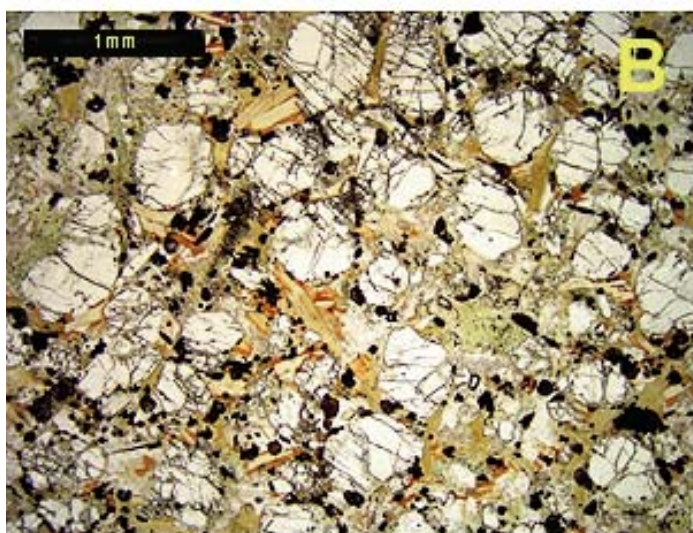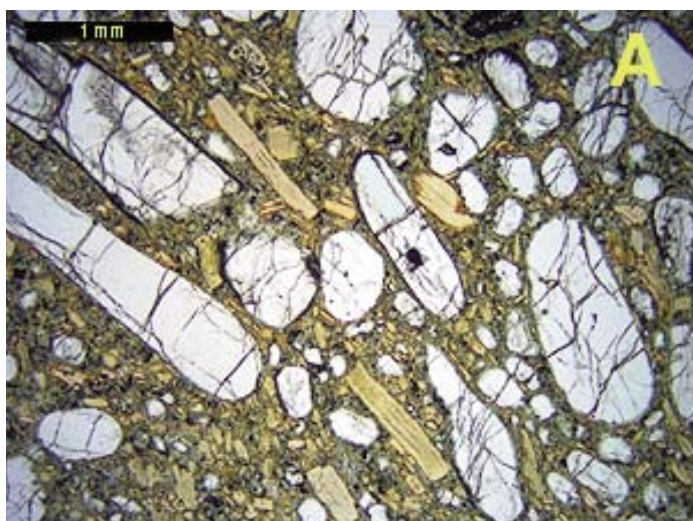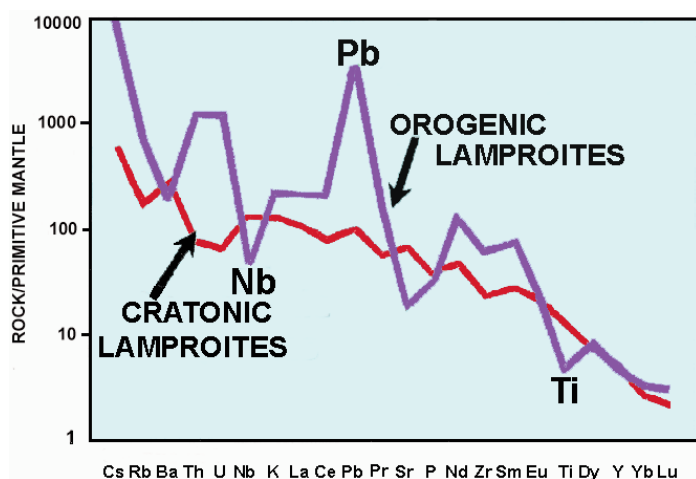
Figure 6. Typical trace element signatures of cratonic versus orogenic lamproites illustrating the characteristic positive Pb and negative Nb and Ti anomalies (after Prelević et al. 2008a).
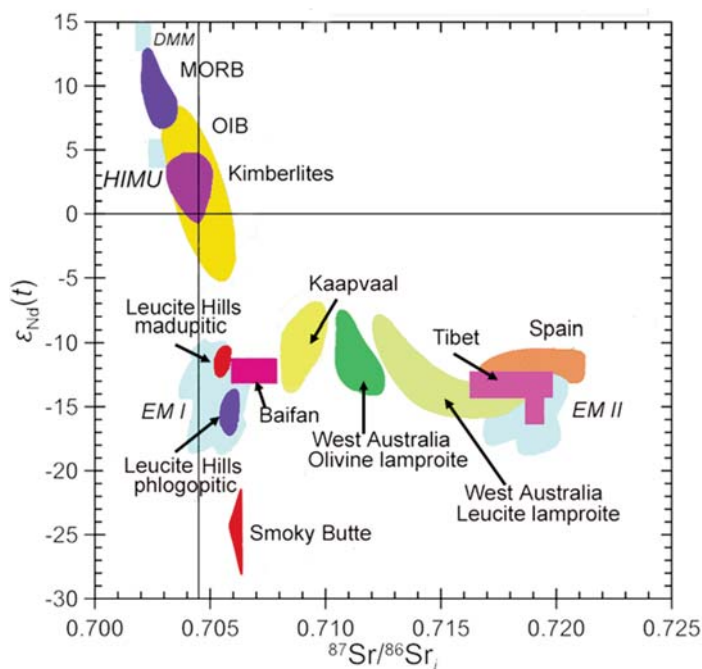

Figure 7. Sr and Nd isotopic signatures of representative cratonic and orogenic lamproites (after Xiang et al. 2020).

al. 1999; Prelević et al. 2008a, b, 2010). The differences are considered to reflect differences in the isotopic composition of the young subducted continental margin sedimentary material involved in their genesis. A major difference between cratonic and orogenic lamproites is their Pb isotopic composition (Fig. 8). The $^{207}Pb/^{204}Pb$ ratios of cratonic lamproites range from

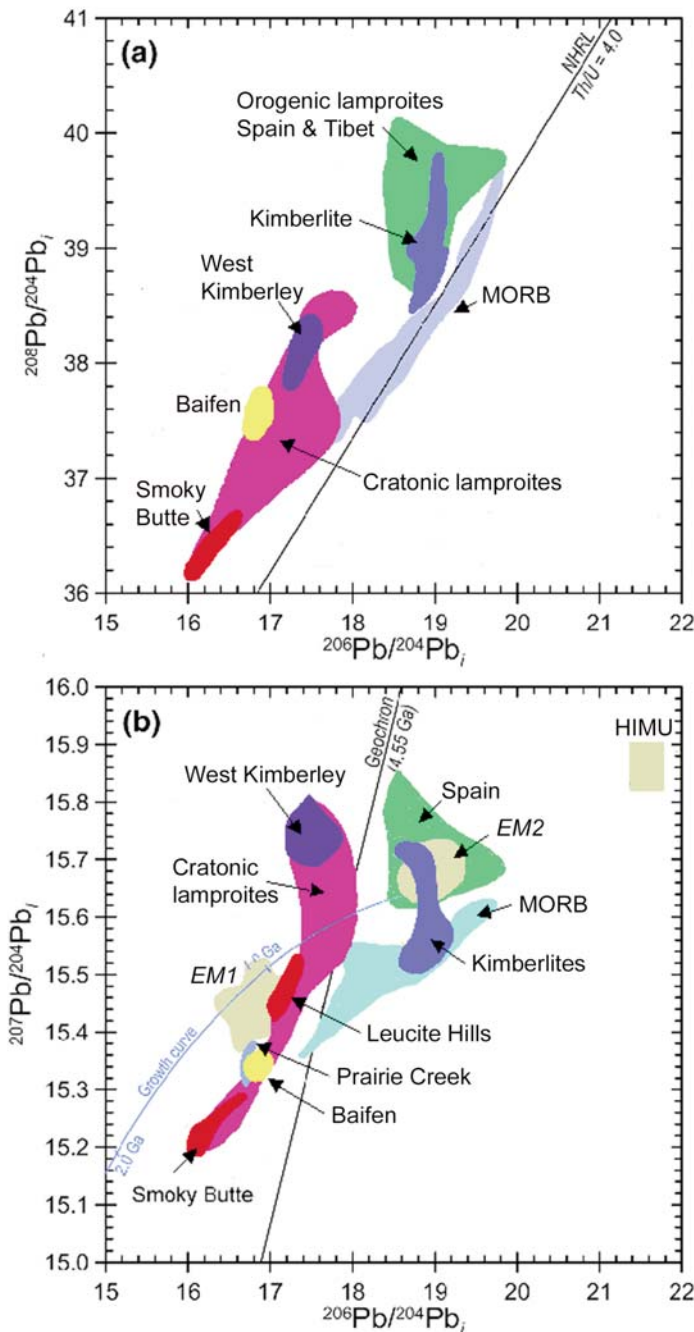**Figure 5.** *(above left)* Examples of olivine lamproite. (A) Macrocrystal phlogopite olivine lamproite from the East Star Fissure Mine (South Africa) with colourless resorbed olivine macrocrysts and pale yellow phlogopite phenocrysts set in a groundmass of phlogopite microphenocrysts, perovskite, chromite, chlorite, and minor carbonate. The margins of many of the phlogopite crystals are altered to red tetraferriphlogopite. (B) Hypabyssal olivine lamproite from Manitsoq (Greenland) with subhedral-to-anhedral olivine macrocrysts set in a matrix of yellow-to-red phlogopite-tetraferriphlogopite, together with opaque perovskite and chromite. (C) Hypabyssal olivine lamproite from Prairie Creek (Arkansas) illustrating primary olivine overgrowths on macrocrystic olivine cores forming a "dog's tooth" texture. The optically unresolved groundmass consists of diopside, phlogopite, perovskite and chromite.

Figure 8. Pb isotopic signatures of representative cratonic and orogenic lamproites (after Xiang et al. 2020).

lamproites (Fig. 7) in exhibiting a very wide range in $^{87}Sr/^{86}Sr$ (0.714–0.722) at near-constant $^{143}Nd/^{144}Nd$ (~ 0.512). Regardless of this similarity, these isotopic signatures have very different origins. Whereas the West Kimberley compositions probably represent single stage partial melting of ancient metasomatized cratonic mantle, the orogenic lamproites require recent mixing of different mantle components, namely a lithospheric mantle source contaminated by subducted continental young sedimentary rocks, a convecting mantle component, and a depleted asthenospheric mantle component (Prelević et al. 2005, 2008a, b).

GEOLOGICAL RELATIONSHIPS

Lamproite magmas behave, in terms of their rheology, in a manner very similar to basaltic magmas. Detailed descriptions of the extrusive and intrusive bodies which they form is beyond the scope of this review and can be found in Mitchell and Bergman (1991) and Jaques et al. (1986). Lamproites can be found as: subaerial vesicular and glassy lava flows (Steamboat Mountain, Zirkel Mesa, Wyoming); lava lakes (Ellendale, Australia); cinder cones (Emmons Cone, Wyoming); lava tubes (Steamboat Mountain, Wyoming); diverse pyroclastic and volcaniclastic rocks (Prairie Creek, Arkansas; Majhgawan, India; Argyle, Australia); differentiated sills (Rice Hill, Australia; Cancarix, Spain); and hypabyssal dyke swarms and minor intrusions (Sisimiut and Manitsoq, Greenland; Smoky Butte, Montana; Raniganj, India). Because of the small volumes of lamproitic magmas, e.g. for the Leucite Hills it is estimated that the total volume of erupted magma is only ~ 0.66 km³ (Lange et al. 2000), they do not appear to form large intrusions of plutonic rocks and the only known pluton is the small (2.7 x 2.5 km; 5–10 km³) Walgidee Hills intrusion, Australia (Jaques et al. 1986, in press).

Many pyroclastic and hypabyssal olivine lamproites (Fig. 9) are diamond-bearing. Because of their economic relevance, lamproite vents and their associated pyroclastic rocks are some of the more important representatives of the lamproite clan. The principal examples are found in: the West Kimberley region of Australia (Ellendale Field, Argyle AK1 Mine); Finsch and Lace Mines (South Africa); Prairie Creek (Arkansas); Majhgawan and Atri (India); and the Kapamba Field (Zambia). Although of small volume, many of the hypabyssal Kaapvaal lamproite dykes are significant sources of diamond. Commonly referred to in South Africa as "fissure mines" the principal examples are: the Roberts Victor; Bellsbank; Sover; New Elands; Star; and Swartruggens mines (Field et al. 2008). Elsewhere, relatively poorer diamond-bearing hypabyssal lamproites include the Bobi and Seguela dykes of Côte d'Ivoire and intrusions in the Wajrakarur region of the Eastern Dharwar craton of India. In contrast to the abundance of diamond-bearing lamproites in the African and Indian cratons, lamproites in North America (Smoky Butte, Leucite Hills, Hills Pond) and Greenland (Sisimiut, Manitsoq) are typically barren with only the Prairie Creek Field carrying significant diamond.

Lamproite Vents
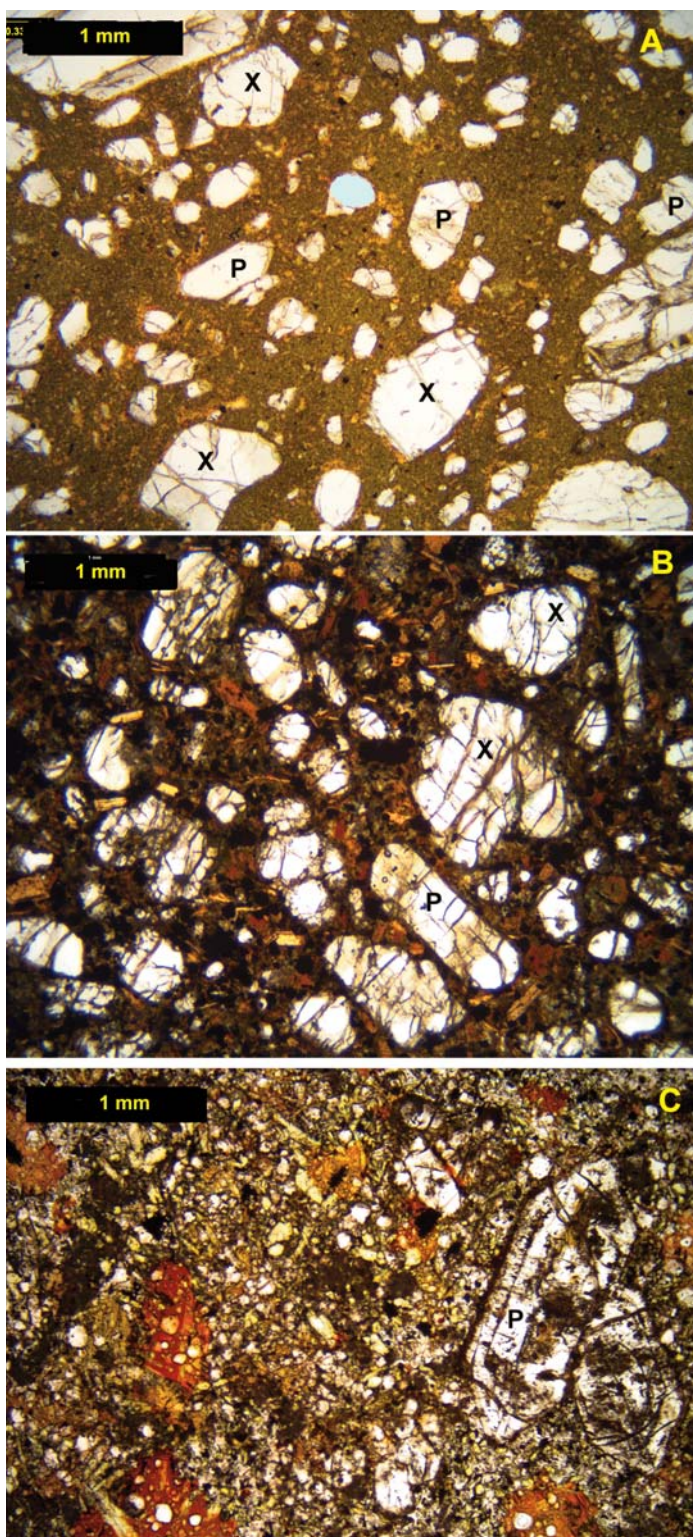The nature of the country rocks into which lamproites are

15.2 to 15.8 and overlap with EM1-type mantle compositions. Orogenic lamproites also exhibit high $^{207}Pb/^{204}Pb$ ratios but have a more restricted range from ~ 15.6–15.85 with overlap with EM2-type mantle. The two groups can be distinguished by the cratonic types having less radiogenic $^{206}Pb/^{204}Pb$ (< 18) and $^{208}Pb/^{204}Pb$ ratios (< 38.6) ratios relative to the more radiogenic $^{206}Pb/^{204}Pb$ (18.5–19) and $^{208}Pb/^{204}Pb$ (> 38.6) signatures of orogenic lamproites (Fig. 8).

Interestingly, the western Mediterranean lamproites have similar isotopic compositions to the West Kimberley leucite

intruded plays a significant role in the style of lamproite magmatism. Lamproite vents with abundant pyroclastic or volcaniclastic rocks are found primarily where the magmas have intruded weakly consolidated sedimentary sequences and where there are significant aquifers. Emplacement in other geological environments results in lavas and/or dykes without pyroclastic sequences. Thus, the major Leucite Hills lamproite province of Wyoming does not contain any pyroclastic or volcaniclastic vents and their expression is as subaerial lavas, monogenetic cinder cones and minor hypabyssal dykes and plugs (Carmichael 1967). Lamproites emplaced in basement crystalline metamorphic rocks typically form dyke swarms, as at Sisimiut and Manitsoq (Greenland).

Although lamproite pyroclastic and phreatomagmatic vents are unlike diatremes formed by Kimberley-type pyroclastic kimberlites they do bear a resemblance to vents formed by the Fort à la Corne-type pyroclastic kimberlites (Scott Smith 2008) as a result of the significant hydrovolcanism involved in the formation of the latter. Because of their economic significance brief descriptions of representative examples of diamond-bearing lamproite occurrences are presented below to illustrate the common factor of phreatomagmatism in their emplacement and the complexities of the geology of these vents.

Argyle AK1 Diamond Deposit, West Kimberley, Australia

The 1180 Ma diamondiferous (30–680 ct/100 t) Argyle AK1 vent was emplaced in Paleo- and Mesoproterozoic sandstone, siltstone, and shale within the Halls Creek orogen at the southeastern margin of the Kimberley craton. Subsequent to emplacement the lamproites were subjected to major and minor faulting. The bulk of this elongate steep-sided NNE-trending deposit (~ 47 ha) consists of pyroclastic or volcaniclastic olivine lamproite intruded by minor late-stage olivine lamproite dykes.

Exploration and mining (Jaques et al. 1986; Boxer et al. 1989; Rayner et al. 2018) have shown that AK1 is a composite body consisting of a large Southern Vent (or diatreme) with two feeder zones, a smaller two phase Northern Vent, and a small elongated unit known as the Southern Extension (or Tail). In outcrop (Fig. 10), the lamproites of the Northern Vent narrow southwards from 500 m in the north to a width of ~ 150 m where they are offset from the Southern Vent by the major sinistral NNW-trending Gap Fault system. South of this fault the main part of the deposit consisting of the Southern Vent(s) extends a further ~ 750 m until it is terminated by the Razor Ridge Fault. This dextral fault has displaced the lamproites to the west as the 400 m x 50 m Southern Extension unit.

The AK1 deposit consists of volcaniclastic olivine lamproites, commonly referred to as "sandy tuffs" and "non-
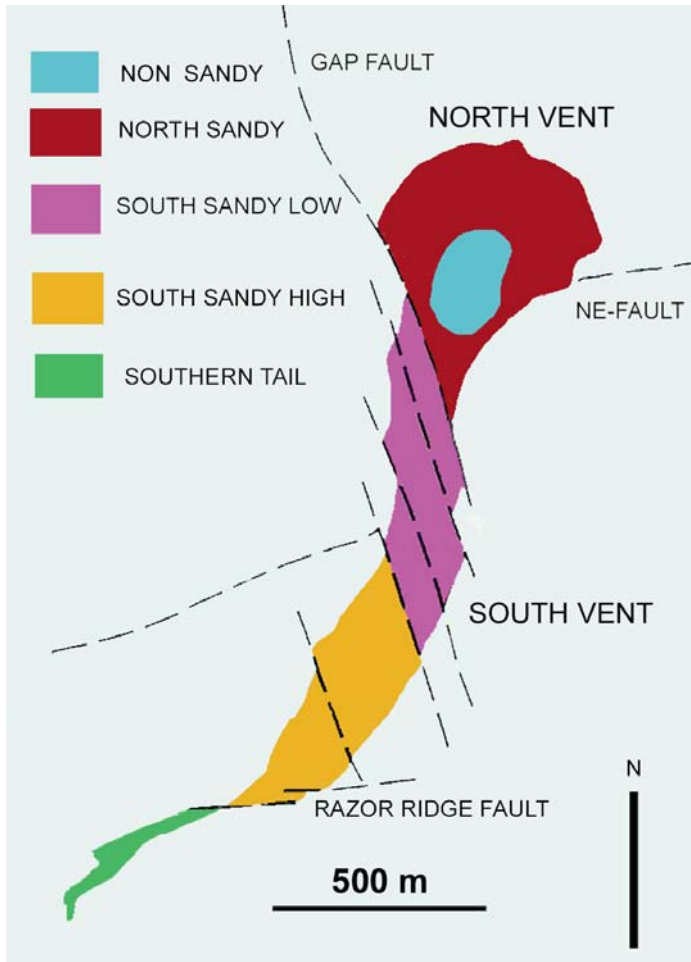
Figure 9. *(above left)* Representative olivine lamproites. (A) Ellendale olivine lamproite with macrocrysts, or xenocrysts (X) of anhedral olivine with minor euhedral primary olivine microphenocrysts (P). The optically, essentially unresolvable, groundmass contains fine-grained diopside, priderite and chromite with poikilitic yellow Ti-phlogopite. (B) Sisimiut olivine lamproite (West Greenland) with olivine macrocrysts/xenocrysts (X) and primary olivine (P) and microphenocrysts of yellow Ti-phlogopite set in a groundmass with diopside microlites and red Ti-phlogopite-tetraferriphlogopite. (C) Madupitic olivine lamproite from Majhgawan (India) with mantled primary olivine phenocrysts (P) set in groundmass with microlitic diopside, altered leucite, chromite in poikilitic red–yellow pleochroic Ti-phlogopite.

Figure 10. Outcrop map of the Argyle AK1 lamproite showing the mining domains (after Roffey et al. 2018).

Figure 11. Representative examples of "sandy tuffs" or volcaniclastic phlogopite olivine lamproites from Argyle AK1 (A) and Ellendale Seltrust Pipe 3 (B). Q = quartz xenocryst; X = country rock xenoliths; L = olivine lamproite clasts; PL = phlogopite olivine lamproite clasts; VL = vesicular olivine lamproite clast. Note that the quartz xenocrysts are rounded, a morphology suggesting that the sandstone was not consolidated at the time of intrusion.

sandy tuffs", on the basis of the presence or absence of xenocrystic quartz derived from poorly consolidated country rocks. The bulk of the deposit (Southern Vent, Southern Extension, most of the Northern Vent), consists of sandy tuffs (Fig. 11A) which are correctly termed quartz-rich volcaniclastic olivine lamproite in modern terminology by Rayner et al. (2018). Figure 10 illustrates that the current mining domains of the Southern Vent are divided into low (< 10 ct/t) and high grade (> 10 ct/t) lamproites, representing different episodes of volcanism. The sandy tuffs of the Northern Vent (< 5 ct/t) have been intruded by lapillar and devitrified lapillar tuffs (non-sandy tuffs) consisting of juvenile lapilli and ash of olivine lamproite.

With respect to the sandy tuffs, four main lithological units are recognized: bedded quartz-rich lapilli tuffs, bedded quartz-rich ash tuffs, bedded quartz-rich fine ash tuffs, and massive quartz-rich lapillar tuffs. Detailed descriptions of these units are given by Rayner et al. (2018). The sandy tuffs show extensive variation in components, texture and bedding, but have common characteristics of formation as multiple small volume maar-type eruptions in a phreatomagmatic environment (Jaques et al. 1986; Boxer et al. 1989).
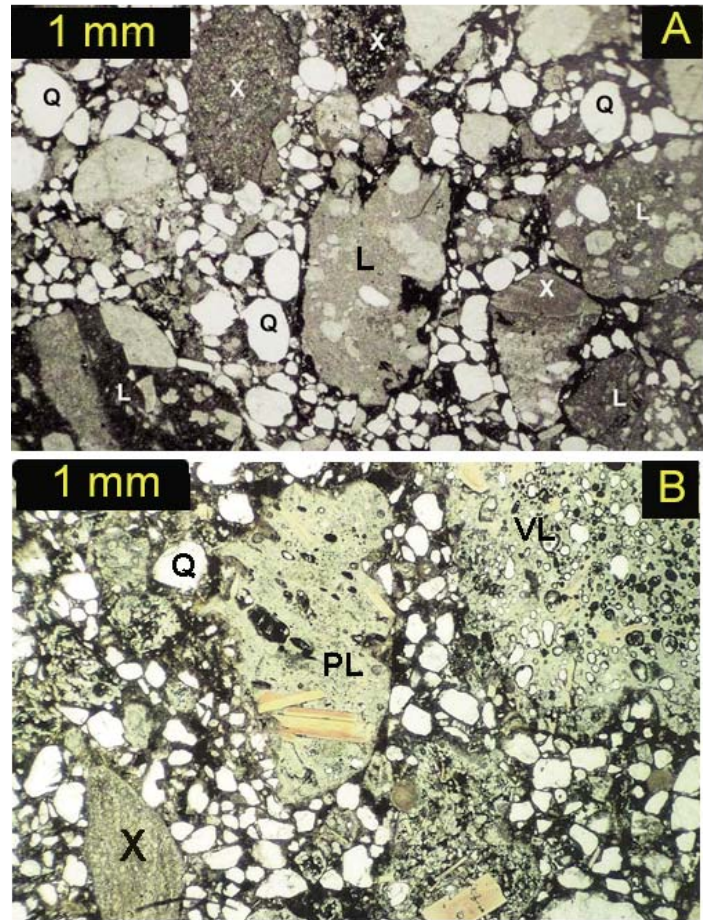
In common with other lamproite vents, initial phreatomagmatism resulted from ascending magma interacting with water-saturated sedimentary units in a fault zone. Maar-type volcanism probably occurred at progressively deeper levels leading to crater formation and coalescence of vents along the main fracture zone. Collapse of rim pyroclastic deposits into the vents resulted in interbedded resedimented and primary volcaniclastic olivine lamproite. The current presence of bedded pyroclastic layers at deep levels (1200 m) in the AK1 vents suggests that continuous subsidence of the vent fill occurred. During the final stages of activity, olivine lamproite magma was erupted into the Northern sandy tuffs. The textures and alteration of the olivine lamproite lapilli forming these non-sandy tuffs resemble those of hyaloclastite, suggesting eruption into a crater lake (Boxer et al. 1989). In contrast to the Ellendale Field (see below), lava lakes were not formed at Argyle, this being a direct consequence of the differences in the character of the country rocks.

Ellendale Field, West Kimberley Province, Australia

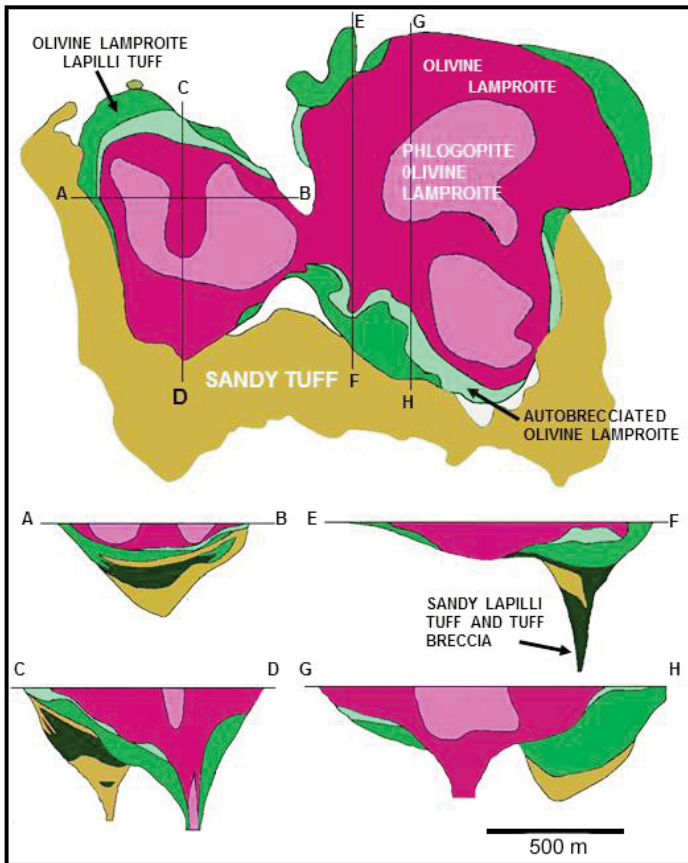The 45 lamproite volcanic centres of the 22–20 Ma Ellendale

Figure 12. Morphology of a typical lamproite phreatomagmatic vent (Ellendale 4, West Kimberley Province) with subaerial pyroclastic "sandy tuffs" of phlogopite olivine lamproite and the vent filled by holocrystalline magmatic olivine lamproite as lava lakes (after Jaques et al. 1986).

Figure 13. Cross-section of lamproite vents in the Prairie Creek Province (Arkansas) illustrating the differential exposure of four volcaniclastic phreatomagmatic vents (VL) as a result of post-emplacement erosion. Hypabyssal olivine lamproite (HL), emplaced in lamproite breccia, is exposed only adjacent to the Little Missouri River system in the Crater of Diamonds vent at the southwestern margin of the field. Vents with lesser degrees of erosion of the Lower Cretaceous country rocks are either hidden under later deposited Upper Cretaceous sedimentary rocks (Twin Knobs) or poorly exposed (Black Lick) at the southern margins of the large essentially un-exposed American Mine vent system. The American Mine was originally worked as scattered exposures in the overlying Tokio Formation. Note that the vertical scale is in feet.

Lamproite Field (Jaques et al. 1986) range from single vents (81 Mile Vent, Ellendale 9) to complex multiple vents (Ellendale 4; Fig. 12). The intrusions in this field exhibit a wide range of morphology and mineralogy ranging from unexposed diamondiferous (< 1–14 ct/100 t) olivine lamproite through phlogopite lamproite as columnar-jointed eroded vents (Mt North) to leucite K-richterite diopside lamproite forming differentiated sills (Rice Hill). The field includes the highly evolved Waldigee Hills pluton characterized by the presence of abundant coarse-grained K–Ti-richterite, noonkanbahite, wadeite, priderite, jeppeite, haggertyite, apatite, Sr-perovskite (Jaques et al. in press).

The vents originate where dykes intruded poorly consolidated sedimentary rocks and aquifers of the Lower Permian Grant Group sandstone. An initial explosive phase produced laminated and bedded olivine lamproite tuffs (Fig. 11B) similar to the sandy tuffs found at Argyle AK1 (Fig. 11A). However, phreatomagmatism was not prolonged, as at Argyle, due to the smaller amount of poorly consolidated sedimentary rocks present in this area. The laminated tuffs consist principally of fractured quartz grains, ash-sized lamproite clasts, phlogopite flakes, and interstitial very finely comminuted lamproite ash (Fig. 11B). The bedded tuffs are airfall deposits similar to those
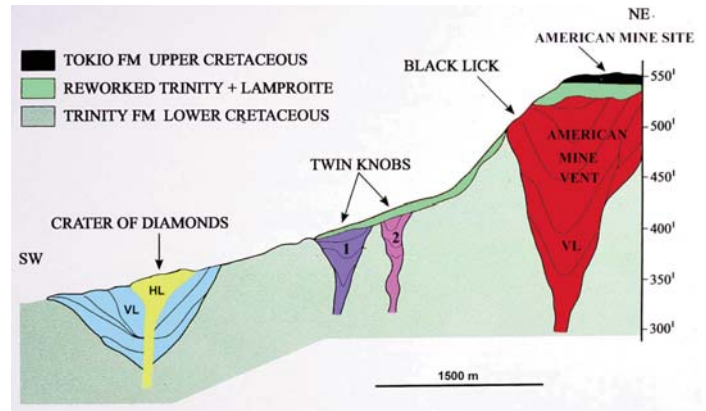
associated with maar-type phreatomagmatic volcanism and consist of rounded quartz grains together with shale and lamproite clasts. The subsequent stages of activity in many of the occurrences are marked by intrusion of holocrystalline hypabyssal-like phlogopite, leucite and olivine lamproites into the tuffs with, in some instances, the formation of lava lakes in former craters.

Prairie Creek Field, Arkansas, USA

The 106–97 Ma Prairie Creek lamproite field (~13 ct/100 t) consists of several lamproite vents emplaced along a northeast–southwest-trending fracture zone into nearly flat-lying Carboniferous–Cretaceous sedimentary rocks (Meyer 1976; Mitchell and Bergman 1991; Dunn 2002). The field includes the Prairie Creek intrusion, also known as the Crater of Diamonds, the only known North American source of lamproite-derived diamonds. All vents contain pyroclastic rocks and hypabyssal olivine lamproite. Figure 13 illustrates how these lamproite vents, belonging to the same magmatic event, appear when subjected to various degrees of erosion. Significant erosion by the Little Missouri River has exposed the lower part of a vent, now represented by the Crater of Diamonds, exposing hypabyssal olivine lamproites (Fig. 1C) and diverse tuff breccias. In contrast, the upper levels of vents, characterized by diverse pyroclastic rocks, are preserved where there has been less erosion. The pyroclastic rocks are typically bedded (Fig. 14) with well-sorted and graded intervals of lithic tuff, and tuff breccia composed of fragments of country rock and juvenile phlogopite, and/or olivine lapilli set in a chloritic matrix with abundant xenocrystic quartz (Fig. 15). The abundance of quartz indicates eruptive disaggregation of the poorly consolidated country rock of the Jackfork sandstone, a member of the Trinity Formation, at depth.
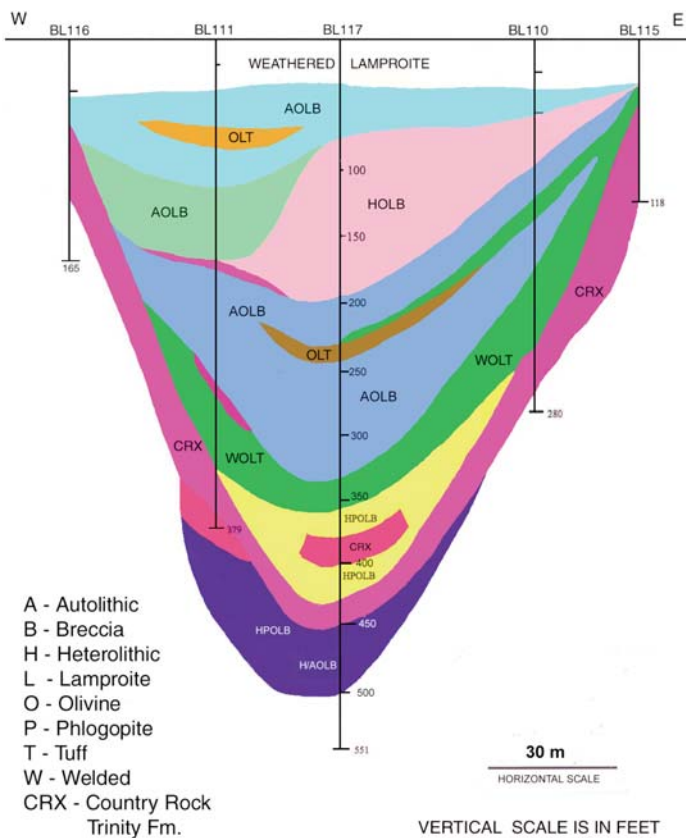
Figure 14. Geological cross-section of the Black Lick-American Mine pyroclastic vent (Prairie Creek Province) illustrating the complexity of the pyroclastic olivine lamproite tuff and breccia sequences. Each unit differs with respect to the abundance of country rock xenoliths, quartz xenocrysts, texture and style of alteration of olivine lamproite clasts. At this structural level hypabyssal lamproites are not present, although a feeder dyke is inferred on the basis of Figure 13 to occur at depth. (data courtesy of Star Resources and Iain F. Downie).

Figure 15. Volcaniclastic olivine lamproite tuffs from the Black Lick Vent (Prairie Creek Province). (A) heterolithic olivine lamproite tuff/breccia with relatively fresh olivine lamproite clasts. (B) quartz-bearing heterolithic olivine lamproite breccia ("sandy tuff") with extremely altered olivine lamproite clasts.

Finsch Mine, Northern Cape Province, South Africa

The 118 Ma diamond-bearing ($\sim$ 37 ct/100 t) rocks forming the cluster of dykes (Smuts, Botha and Bonza) and vents (Finsch, Shone, Bowden) were for many years considered to be kimberlite but are now recognized as *bona fide* lamproite. Unfortunately, the designation as Group 2 kimberlite persists in many publications concerned with diamond deposits (e.g. Field et al. 2008). The lamproites were intruded into the Proterozoic Griqualand West dolomite, banded iron formation, and shale. The Finsch mine occurs as a vent on the northeast-striking Smuts Dyke and consists of eight (F1–F8) main lamproite types (Clement 1982). Ekkerd et al. (2006) have described the sequence of emplacement and presented representative descriptions of the individual intrusions. The Finsch vent (Fig. 16) consists principally of phlogopite lamproite and diopside phlogopite lamproite breccia containing xenoliths of Karroo basalt and Griqualand West sedimentary rocks which have been intruded by hypabyssal phlogopite lamproite as a central body and as internal dykes and sills. Karroo-age rocks were present at the time of emplacement but have subsequently been removed by erosion.

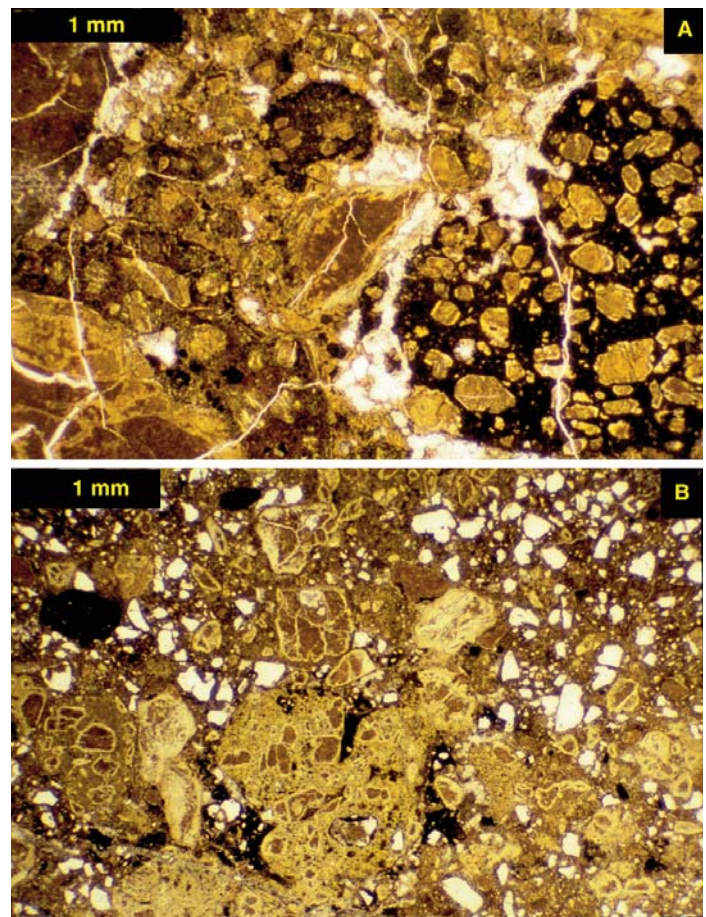Finsch hypabyssal lamproites are olivine phlogopite lamproites with serpentinized rounded olivine crystals set in a matrix of phlogopite laths, in turn set in a matrix of mica plates, microlitic diopside. perovskite, apatite, and spinel of various compositions. The Finsch F1 volcaniclastic lamproite is the most abundant unit and of similar mineralogy to the hypabyssal units, apart from the presence of abundant xenolithic material. The F8 lamproites are unusual in that large round lamproite magmaclasts similar to those occurring in the Pilot Butte lamproites and some Kimberley-type pyroclastic kimberlites (Mitchell 1997) are present.

Majhgawan, Madhya Pradesh, India

The diamondiferous Majhgawan volcaniclastic lamproites (ca. 7–19 ct/100 t) were intruded (ca. 1080–1067 Ma) into sandstone and shale of the Proterozoic Vindhyan Supergroup which were deposited at the southeastern margin of the Archean Bundelkhand Craton. At the current level of erosion the Majhgawan vent is exposed in the Kaimur Group sandstone and the overlying Rewa and Bhander groups, which are considered to have been present at the time of intrusion, and now found as xenoliths in the lamproite (Fareeduddin and Mitchell 2012).

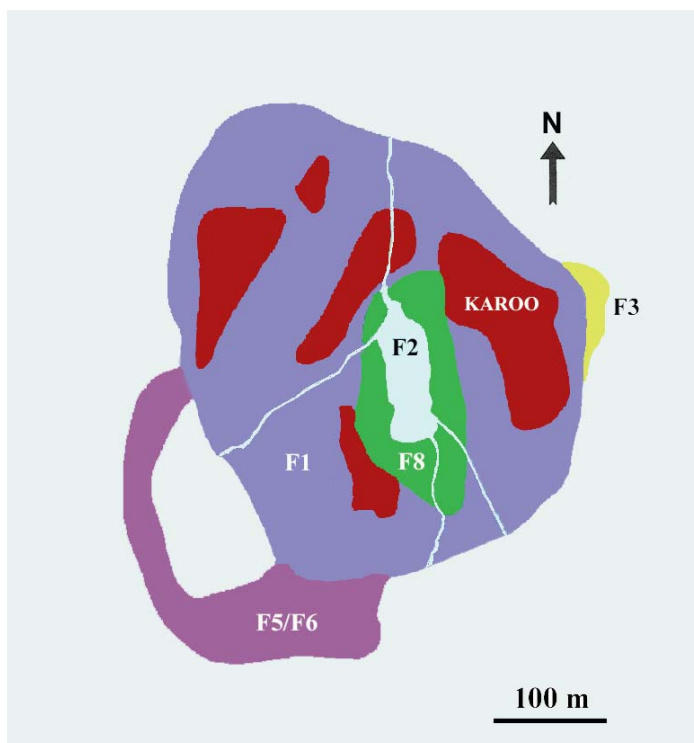The Majhgawan vent has been interpreted as a downward tapering cone-shaped body with a pear-shaped outcrop meas-

Figure 16. Plan view of the Finsch Mine lamproite, South Africa at the 510 m level showing the distribution of the diverse petrographic varieties of the lamproite and the presence of megaxenoliths of Karoo age sedimentary rocks (after Ekkerd et al. 2006).

uring 530 x 320 m. Recent drilling has shown that the vent is reduced in cross-section to about 125 m at depth of 330 m, suggesting that the volcaniclastic rocks originated from a hypabyssal feeder dyke emplaced in the Bundelkhand granite. The smaller (200 x 180 m) adjacent Hinota vent is considered to have been formed by a branch of this feeder dyke. The geology and mineralogy of this satellite vent is not well characterized as it appears to have no economic potential.

Regardless of the antiquity of mining, the geology of the Majhgawan vent is not well-understood, in part, due to the paucity of exploration drilling and the intermittent character of mine operations. Models presented by Mathur and Singh (1971) and Rao (2007) have suggested the vent consists of concentric bands of volcaniclastic rocks all of which taper to a common focal point at unknown depth. Given the complexities of other lamproite vents, in particular the Atri Pipes (see below; Das et al. 2018), revealed by recent studies, such a model is highly improbable and should be re-evaluated. The vent fill consists of diverse heterolithic olivine lamproite breccias distinguished on the basis of colour, grain size, content of xenoliths, and abundance of mica (Fig. 17). The margins of the vent on the east and west sides are different varieties of breccia, and the finer grained core is an intensely brecciated mica-free lamproite. The breccias contain clasts of vesicular pyroclastic lamproite (see below).

Interpretation of the geology and petrology of the vent has been hampered by the incorrect designation as "kimberlite", "transitional kimberlite", "orangeite", or "majhgawanite"
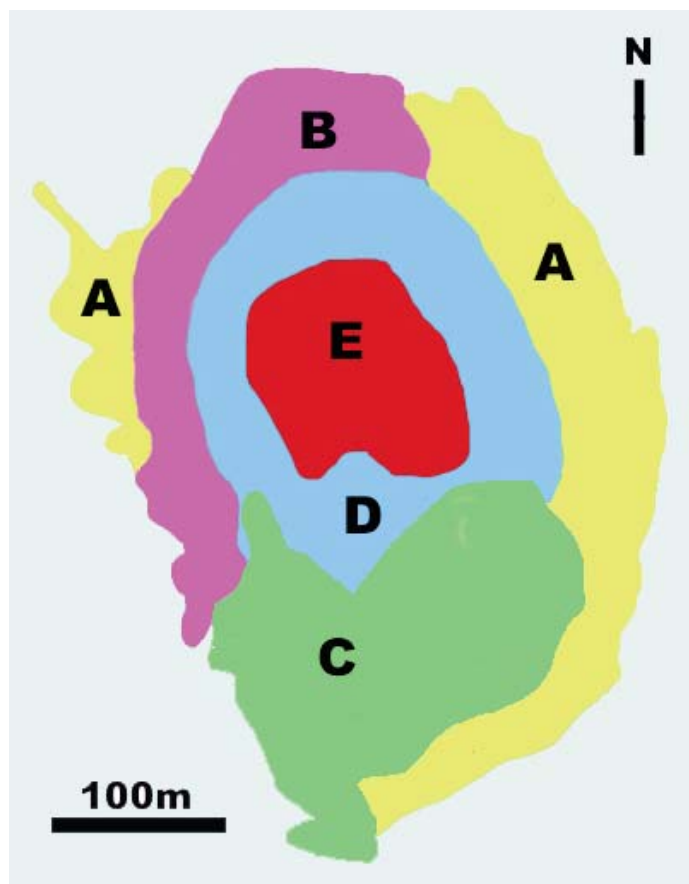

Figure 17. Outcrop plan of the Majhgawan lamproite illustrating the disposition of the pyroclastic units (after Mathur and Singh 1971; Rao 2007). A = yellow-green heterolithic pyroclastic breccia; B = yellow-brown heterolithic pyroclastic breccia; C = heterolithic breccia; D = mica-rich pyroclastic breccia; E = mica-free breccia. Note that these units require re-investigation and reclassification (see Fig. 18).

(Chalapathi Rao 2005), regardless of the correct classification as lamproite by Scott Smith (1989). This study was the first detailed investigation of the breccias and revealed the presence of glassy and vesicular juvenile lapilli (Fig. 18), and the presence of olivine lamproites similar to those found elsewhere. The mineralogy and texture of lapilli forming the breccias are typical of olivine phlogopite lamproites in general with mica phenocrysts set in a groundmass of Al-poor mica, Ti-spinel, rutile, perovskite, and a wide variety of secondary minerals (Fig. 18). As the mineralogy and petrology of the vent rocks are not well understood a complete re-investigation of the Majhgawan lamproites by modern methods is required. What is evident from the limited studies is that most of the vent rocks are pyroclastic in origin and similar to pyroclastic lamproites occurring in the nearby Atri Pipes (see below). Thus, the geology and economic evaluation should be interpreted using airfall eruptive and phreatomagmatic models similar to those proposed for the Atri, Argyle and Ellendale pyroclastic lamproites.

Saptarshi Lamproites and the Atri Pipes, Madhya Pradesh, India

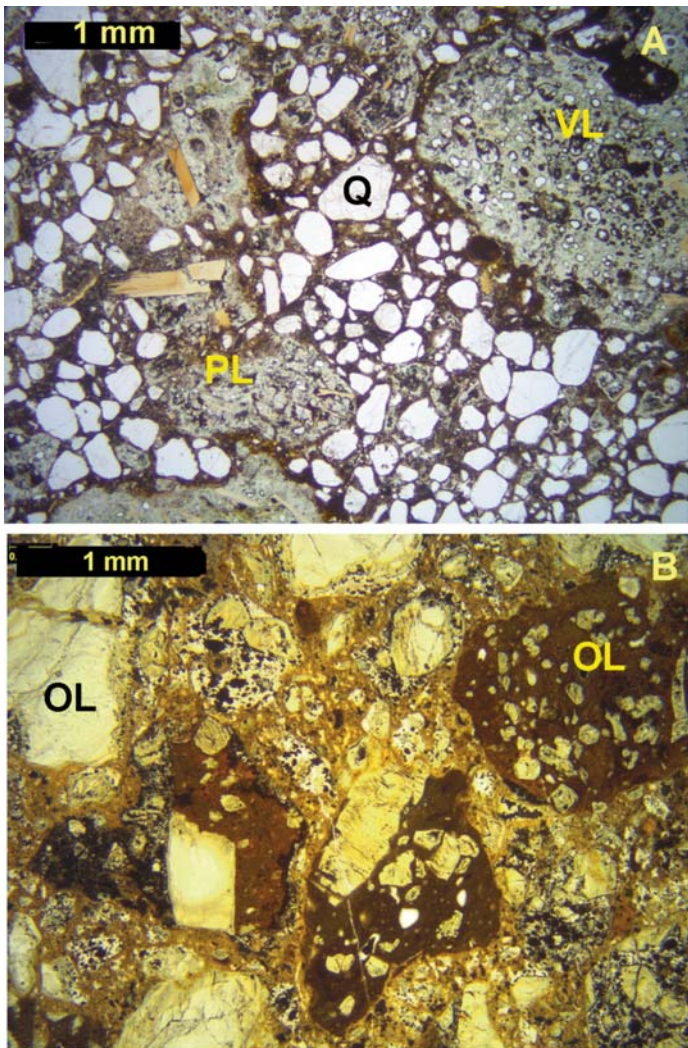The Saptarshi Lamproites, discovered in 2004 by Rio Tinto's

Figure 18. Volcaniclastic lamproites from Majhgawan Mine (India). (A) Quartz-rich tuff (or "sandy tuff") with vesicular juvenile lamproite clasts (VL) and fine-grained phlogopite lamproite (PL) clasts. Note the close petrographic similarity of this lamproite to the Seltrust Pipe 3 lamproite illustrated in Figure 11B. (B) Olivine lamproite tuff-breccia with clasts of altered hypabyssal olivine lamproite. Note the close similarity of this lamproite to the olivine lamproite tuff-breccia from the Black Lick vent (Arkansas) illustrated in Figure 15A. These similarities indicate that the Majhgawan tuffs are typical lamproite phreatomagmatic volcaniclastic rocks similar to those occurring at Argyle AK1 and Atri, and are not kimberlites.

Bunder Diamond Project (Das et al. 2018) are a cluster of seven lamproite vents and dykes located 80 km west-southwest of Majhgawan. The lamproites were emplaced in Vindhyan Kaimur Group supracrustal sedimentary rocks contemporaneously with the 1080–1067 Ma Majhgawan-Hinota vents. The major occurrence is the 1079 ± 6 Ma, Atri Pipe (18.5 ha) which consists of at least two irregular downward-tapering vents (Atri North and South) of diamondiferous pyroclastic/volcaniclastic lamproite (44 Mt @ 0.7 ct/t) which have coalesced near the present surface where Atri North cross-cuts Atri South (Fig. 19).

Five distinct lamproite pyroclastic or volcaniclastic units are present in the South pipe and three in the North pipe. These lamproites, described in detail by Masun et al. (2009)
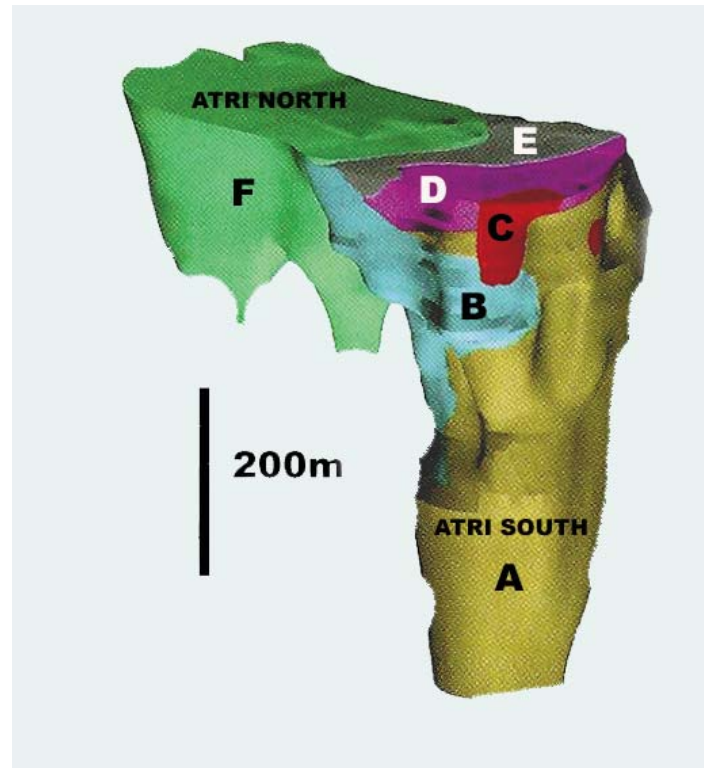

Figure 19. Model of the geology of the Atri lamproite vent looking northeast (after Das et al. 2018), showing the disposition of pyroclastic units in the South (A–E) and North (F) lamproites. Individual units in the northern vent are not delineated, and this vent is interpreted by Das et al. (2018) to have several feeders.

and Das et al. (2018), consist of diverse melt-bearing olivine phlogopite pyroclasts with country rock clasts and rarer autolithic clasts. Individual units (Fig. 19) can be easily distinguished on the basis of texture, colour, xenolithic, and primary mineral constituents. The rocks are similar to the Majhgawan lamproites and contain many vesicular pyroclasts. Mica compositions follow the lamproite trend of compositional evolution from phlogopite to tetraferriphlogopite with Ti- and Al-depletion coupled with Fe^{3+} enrichment (Das et al. 2018).

Unfortunately, regardless of the mineralogical and petrological evidence, Das et al. (2018) have incorrectly classified the Atri Pipes as "transitional kimberlite-orangeite-lamproite" or "majhgawanite". As noted above this nomenclature is petrogenetically impossible and should be discontinued. Both the Bunder and the Majhgawan pyroclastic/volcaniclastic rocks are *bona fide* lamproites derived from metasomatized lithospheric mantle, which can also be termed lamproite (*var*. Bundelkhand) following Mitchell (2006).

Das et al. (2018) considered that the Atri vents are composed predominantly of pyroclastic rocks with the low modal abundances of country rock xenoliths suggesting that pipe excavation preceded vent in-filling. The products of these events are not preserved at the current level of erosion. At Atri North several airfall pyroclastic eruptions of varying intensity and volume occurred, which included the formation of graded beds. The Atri South vent represents a change in locus of eruption and eruptive products and included the formation of units with graded beds, cross-beds, and soft sediment defor-

mation. The lamproites are finer grained and probably represent a phreatomagmatic style of eruption.

PETROGENESIS

A comprehensive review of the petrogenesis of lamproites is well beyond the scope of this work as it would require a detailed discussion of metasomatism and the mineralogy of the lithospheric mantle; how experimental petrology and isotope geochemistry has led to an understanding of differences in the formation of the sources of lamproites; the relative roles of mantle metasomatism and/or ancient and recent subduction; depth, causes and styles of melting leading to lamproite magmatism; and the tectonic history of particular cratons and orogenic belts containing lamproites. Summaries of these topics can be found in Mitchell and Bergman (1991) and Mitchell (1995a).

As each lamproite province is mineralogically and geochemically different, and lamproite magmas are neither common nor abundant, it is evident that there cannot be a single simple petrogenetic scheme applicable to all lamproites, although all have in common origins from metasomatized lithospheric mantle sources. Unlike common magma types, their genesis and composition are not repeated uniformly in time and space. *Thus, the formation of each lamproite province must be regarded as a singular event without the possibility of re-occurrence or formation of another province of identical character.* The rarity of lamproites also suggests that processes leading to their formation are also very rare and require particular tectonic environments and melting regimes. Thus, apart from the general observation that cratonic and orogenic lamproites appear to have different origins, the genesis of each lamproite province must be evaluated on its own merits. For details of many of these aspects of lamproite genesis see: Mitchell and Bergman (1991); Foley (1992a, b); Conticelli and Peccerillo (1992); Mitchell (1995a); Conticelli et al. (2002); Prelević et al. (2010); Krmíček et al. (2016); and Helmstaedt (2018).

The most important process in the petrogenesis of lamproites is the development of their lithospheric mantle sources. The initial stage appears to be formation of harzburgitic depleted mantle by extraction of large volumes of basic magma. A second stage requires the addition of incompatible elements to this substrate (Foley 1992a, b). This process is one of the more speculative aspects of lamproite genesis as it is not resolved as to whether incompatible element-rich fluids or melts originate from the asthenosphere, are introduced by partial melting of subducted material, or result from a combination of these processes. From isotopic data, experimental studies of lamproites at high pressure, and the mineralogical character of mantle xenoliths such as the MARID suite (mica–amphibole–rutile–ilmenite–diopside rocks, Dawson and Smith 1977) and metasomatized harzburgite, it is clear that harzburgite substrates must contain modally significant quantities of minerals that can sequester significant amounts of incompatible elements rather than these occurring as trace elements in common mantle minerals (i.e. cryptic metasomatism). The development of these new mineral assemblages is termed patent metasomatism and results in the formation of modally diverse veins in the harzburgite substrate (Foley 1992a, b).

The mineralogy of the metasomatic veins, or metasomes (Haggerty 1989), is considered to be dominated by minerals which can sequester K, REE, Ti, Ba, Sr, Zr, Nb, P, and volatile elements. The major components are probably titanian phlogopite and K-titanian richterite, the principal components of MARID xenoliths, both of which are stable throughout the lithospheric mantle and also at depths of up to 300 km. Other potential phases that have been recognized from mantle-derived xenoliths are: diopside; Nb-rutile; Cr–Mg-ilmenite; lindsleyite–mathiasite, yimengite–hawthornite; hollandite group K–Ba–V titanate minerals (priderite, redledgite, mannardite); and wadeite (Haggerty 1995). Experimental studies of the crystallization of potential primary lamproite magmas at lithospheric mantle pressures (4–8 GPa) suggest the presence of Zr-bearing $K_4(Si,Ti)_9O_{20}$, K–Ba-phosphate, Sr-apatite, and K-feldspar in the metasomes (Mitchell 1995b). The presence of apparently primary calcite in the Kaapvaal and Raniganj lamproites is unusual and its source from asthenospheric melts, pre-existing lithospheric primary carbonate or subduction is unknown. Although some carbonate-bearing lamproites are also known from West Kimberley, the primary source of this carbonate appears to be contamination by local limestone country rocks but it is possible that late calcite veins in the centre of the Walgidee Hills are deuteric (Jaques et al. 1986).

It is to be expected that the mineralogy of metasomatically enriched mantle will not everywhere be identical and that modal variations will lead on a long-term basis (gigayears) to the different isotopic compositions reported for lamproites (Figs. 7 and 8). Apart from the inherent modal variations of the veins, melting in harzburgite substrates according to the vein–wall rock partial melting models of Foley (1992b), will also give rise to unique magma compositions depending on the ratio of vein (V) to wall rock components introduced as melts (W) or xenocrysts (WX). Mitchell and Bergman (1991) and Mitchell (1995a, b) considered that silica-rich erupted phlogopite lamproites, such as occur at North Table Mountain and Steamboat Mountain (Leucite Hills) or Smoky Butte (Montana), represent the closest approach to primary magmas (Table 2) and represent partial melts in which vein components are dominant with V/(W +WX) ratios greater than 50%. Similar high vein contributions can be postulated for other un-evolved silica-rich phlogopite lamproites such as found at the Ellendale 81 Mile Vent (Table 2). Following eruption of these magmas, differentiation by crystal fractional of liquidus phases leads through lamproites with leucite and diopside phenocrysts to evolved lamproites with groundmass tetraferriphlogopite, K–Ti-richterite and K-feldspar. In contrast, olivine lamproites are demonstrably hybrid rocks contaminated by wall-rock-derived olivine. Initial melts must have had low V/(W+WX) ratios (< 5%) with olivine apparently dominating the WX fraction. The absence of orthopyroxene xenocrysts is unexpected for partial melts derived from a harzburgite substrate and is a feature in common with kimberlites contaminated by mantle material (Mitchell 1997; Mitchell et al. 2019). Only a few silica-rich lamproites from Spain (Fortuna, Cancarix) and the Leucite Hills (Emmons Cone) contain orthopyroxene. These are typically Fe-rich relative to harzburgite orthopyroxene and consid-

ered to be xenocrysts or bronzite–mica microxenoliths (Mitchell and Bergman 1991). Not surprisingly olivine lamproites do contain mantle-derived orthopyroxene-bearing xenoliths of garnet lherzolite and harzburgite (Jaques et al. 1986; Dunn 2002). The typical absence of orthopyroxene in olivine lamproites can be explained by its incongruent melting which produces silica-rich liquids plus crystallization of the current liquidus phase, which in these melts is probably olivine and/or phlogopite. Hence, again in common with kimberlites, some olivine crystals are interpreted to be xenocrysts whereas others are primary phases. The combination of these parageneses can be seen in the formation of "dog's tooth"-textured olivine (Fig. 5C) in some olivine lamproites. Note that the sequence of crystallization of the groundmass of olivine lamproites leads to mineral assemblages similar to those observed in evolved lamproites implying that even initial melts with low V/(W+WX) ratios were also incompatible element- and silica-rich. Given that only olivine lamproites contain xenocrystic diamond it is not a coincidence that they are also the only lamproite magmas extensively contaminated by lithospheric mantle. These magmas might be melts formed in parts of the mantle containing few metasomatic veins or are initial melts in peripheral regions of extensively modified mantle. What is certain is that they are not primary magmas to phlogopite lamproites and their evolved derivatives.

As noted, the origins of enriched metasomes in many instances have not been conclusively identified and diverse hypotheses have been advocated for both these and the tectonic factors leading to the initiation of partial melting of the mantle for individual lamproite provinces. Although detailed discussion is well beyond the scope of this work some examples illustrating the diversity of opinion are given below.

Leucite Hills Province
The 3.0 to 0.89 Ma Leucite Hills lamproites (Carmichael 1967) are typical of cratonic lamproites in being emplaced near the margin of the Archean Wyoming craton about 100 km north of the surrounding Cheyenne mobile belt which separates the craton from the Colorado Plateau. The genesis of the province initially involved Archean craton formation resulting in a residual harzburgite lithospheric mantle which underwent subsequent metasomatism. The origins and age of this metasomatism have not been constrained and are considered to range from the Archean (3.2–2.5 Ga) to several Proterozoic events ranging from 2.5–1.0 Ga (Vollmer et al. 1984; Mirnejad and Bell 2006). The presence of negative Nb, Ti, and Ta anomalies in the trace element distribution patterns and the isotopic composition of the lamproites are considered by Mirnejad and Bell (2006) to indicate involvement of subduction in these events rather than any sub-lithospheric sources. Subsequently, the metasomes remained closed systems, for at least 1 Ga, until they were re-metasomatized by volatile-rich material derived from asthenospheric mantle upwelling. Complete partial melting of veins without involvement of the harzburgite substrate resulted in silica-rich melts which were erupted without differentiation during transit through the lithosphere or pooling in the crust. Lange et al. (2000) considered that the time of eruption was closely related to time of melting.

The initiation of the Quaternary lamproite magmatism has been attributed to the peripheral thermal effects of the Yellowstone plume (Mitchell and Bergman 1991); back-arc extension and lithospheric thinning associated with the northwest subduction of the Farallon oceanic plate; or uplift of the Colorado Plateau related to delamination of the lower crust by lithospheric downwelling, together with passive upwelling of the asthenospheric mantle (Levander et al. 2011). Although any relationships with the Yellowstone plume have been effectively ruled out by Lange et. al. (2000) and Mirnejad and Bell (2006), details of the relationships of the Cenozoic lamproite and other magmatism with the subducted Farallon Plate and Colorado Uplift remain unsettled. All models acknowledge the importance of the northwesterly low angle subduction of the Farallon oceanic plate in removal of lithospheric mantle and heating of the base of the Wyoming craton by upwelling asthenosphere (Levander et al. 2011; Hernández-Uribe and Palin 2019).

The Leucite Hills form an isolated province geographically isolated from other alkaline rocks although the genesis of the 40–13 Ma Francis (Moon Canyon) lamproites, located 250 km to the southwest at the margin of the Wyoming craton is also probably related to Colorado Plateau uplift. Minette intrusions are common within the Colorado Plateau and Montana although these are considered to have different sources and genesis to lamproites (O'Brien et al. 1995). Kimberlites are absent from the Leucite Hills Province but do occur in western Colorado, although these are not related genetically, and in addition are of Devonian age.

Kaapvaal Lamproites
The Kaapvaal cratonic lamproites are located in two principal clusters: 165–145 Ma intrusions in the centre, and 125–110 Ma intrusions at the southwestern margin of the Kaapvaal craton, suggesting two discrete episodes of magmatism. Many of the older petrogenetic hypotheses for Kaapvaal lamproites are now regarded as untenable as the lamproites were considered to be part of a broader spectrum of "kimberlite" magmatism. Regardless, most of these hypotheses (e.g. Becker and le Roex 2006; Coe et al. 2008) require for their genesis the formation of ancient enriched metasomes with phlogopite and amphibole at the base of the lithosphere (150–200 km). Recently, Giuliani et al. (2015) have focussed upon the similarity in composition of lamproites and the MARID xenoliths which have been found in both lamproites and kimberlites in southern Africa, and have suggested that MARID suite rocks form the metasomes.

Formation of enriched lithosphere is ascribed to late Proterozoic subduction under the Archean Kaapvaal craton and the accretion of adjacent 1.1 Ga Proterozoic Namaqua-Natal mobile belt with fluids or melts carrying a calc-alkaline geochemical signature into the subcontinental lithospheric mantle (Becker and le Roex 2006; Coe et al. 2008). These metasomes remained closed systems until the break-up of Gondwana (150–144 Ma) by one or more mantle plumes (Becker and le Roex 2006) resulted in partial melting. In contrast to this model, Giuliani et al. (2015) have suggested that the meta-

somes were formed by, and during, earlier (~ 180 Ma) Karroo asthenospheric magmatism. This hypothesis obviates any need for any subducted component in their genesis, although eclogite representing subducted material is common as xenoliths in these lamproites. A problem with this hypothesis is that the time between metasome formation and lamproite genesis might be insufficient to generate the observed isotopic signatures.

Regardless of the causes, partial or complete melting of metasomes, with or without wall rock contributions, following the Foley (1992b) models, resulted in the genesis of olivine lamproites or silica-rich types, respectively. In addition, the formation of Kaapvaal olivine lamproites requires a carbonate component which must be either added to some, but not all, parts of the metasomes during partial melting, or by contamination in the mantle during ascent of particular batches of melt. The origin of this carbonate remains an unresolved problem.

Most earlier studies of the Kaapvaal craton suggested the presence of a thick craton with a "smooth" keel (see Mitchell 1986; Haggerty 1989) and the location of subducted material at the lithosphere–asthenosphere boundary. In contrast, recent geophysical studies (Celli et al. 2020) have shown this simple picture does not describe the current configuration of most African cratons, and that much of the of original Kaapvaal craton, including any subducted components, has been removed by sub-lithospheric erosion. The 180 Ma Karroo large igneous province, the 150–110 Ma lamproites, and the ~ 90 Ma kimberlites, are all now situated over an eroded thinned part of the craton. Erosion and magmatism might be related to a fixed region of asthenospheric upwelling rather than associated with migrating hot spots, as suggested by Becker and le Roex (2006). In such a scenario partial melting of ancient metasomes could be due to melt/fluid influx associated with lithospheric thinning. However, appeal to such Maxwell's Demons is not a satisfactory solution to the problem as the temporal and tectonic relationships between the lamproites, kimberlites, and the earlier Karroo magmatism are not resolved. Clearly, two temporally distinct partial melting events are involved in Kaapvaal lamproite genesis, perhaps involving mineralogically distinct metasomes in different parts of the craton. In addition, many ancient metasomes might have been destroyed and assimilated during craton erosion and the genesis of the Karroo magmas, perhaps accounting for the relatively restricted occurrence of lamproites in contrast to the widespread distribution of younger asthenospheric kimberlites in southern Africa. Recent subduction or rifting is not considered to have played any role in the genesis of Kaapvaal lamproites.

Tibetan Lamproites

Lamproite lavas occur in eight distinct fields in the western region of Lhasa Block (Chen et al 2012) located at the southwestern margin of the Tibetan Plateau. These lamproites were emplaced in an area of active tectonism and illustrate well the complexities of orogenic ultrapotassic magma genesis as, in common with the Spanish and Italian lamproites, they are associated with abundant less potassic rocks, and minor felsic

magmas (Miller et al. 1999; Mo et al. 2006; Gao et al. 2007; Xia et al. 2011; Chen et al. 2012; Guo et al. 2015; Zhang et al. 2017). The lamproites and other potassic rocks represent post-collisional magmatism with emplacement ages of 25–18 Ma and 13–8 Ma, respectively (Miller et al. 1999; Gao et al. 2007). Individual lamproite fields have distinctive geochemical characteristics with high Pb abundances, low Ce/Pb ratios, and Pb isotopic ratios indicative of binary (or ternary) mixing, implying contributions to their genesis from diverse subducted materials and mantle components. Lamproite sources are also geochemically distinct from those of the more widespread potassic volcanism in the Lhasa and Qiangtang Blocks of the Tibetan Plateau (Guo et al. 2015).

Petrogenetic hypotheses for the lamproites are complicated by the diversity of hypotheses proposed for the geodynamic evolution of the Tibetan Plateau which include convective removal of the subcontinental lithospheric mantle, subducted slab roll-back and break-off, and intra-continental subduction. There is an extensive literature on these topics. For recent summaries of the tectonics of the India–Asia collision see, among many others, Ge et al. (2012), Hyndman (2019) or Xiao et al. (2020). As the components and extent of the Indian plate underthrusting and paleothermal regime under Tibet are not well-constrained, lamproite petrogenetic models are at best speculative.

In common with other models of lamproite genesis it has been suggested by Miller et al. (1999) that the Tibetan lithospheric mantle was enriched by a complex multi-stage metasomatism from > 2.2 Ga to 1.3 – 1.9 Ga and remained isolated until recently. The origins of the enriched sources are not well-characterized by Miller et al. (1999). The potassic and lamproitic magmatism is interpreted as the product of partial melting resulting from either convective thinning of the lithosphere with diverse magmas derived from distinctive sources or subducted oceanic plate break-off resulting in the uprise of hot asthenosphere causing thermal perturbations and melting of heterogeneous domains in the lithospheric mantle. In contrast, Gao et al. (2007) claimed that such isolation is unlikely given the complex Phanerozoic tectonic and magmatic evolution of Tibet, and suggested that metasomatism by partial melts from isotopically evolved old sedimentary material subducted with the Tethyan slab can explain the apparent Precambrian Nd and Pb model ages reported by Miller et al. (1999).

Guo et al. (2015) have shown that the Sr–Nd–Pb isotopic compositions of Tibetan lamproite and potassic volcanic rocks define linear trends between depleted MORB, source mantle (DMM) and Indian continental crust. The enrichment of the upper mantle below southern Tibet is considered to result from the addition of material derived from subducted Indian continental crust to the overlying mantle wedge during the northwestern underthrusting of the Indian plate at 55 Ma. In contrast to most lamproite petrogenetic models the post-collisional lamproites are considered to be generated by partial melting of pyroxenite in a mantle source created by reaction of hydrous fluids and silica-rich melt derived from subducted granulite–eclogite facies Indian continental crustal with surrounding peridotitic mantle. Slab roll-back and detachment then induces partial melting of pyroxenite.

Although the Tibetan lamproites are well-characterized in terms of their mineralogy, trace element and isotope geochemistry, it is evident that a geological solution to their genesis remains elusive. This is because of the complexity of the tectonic evolution of the sub-Tibetan lithospheric mantle coupled with underthrusting of the Indian plate which precludes both definitive characterization of potential enriched sources and mechanisms of partial melting. Interpretation of genetic models in terms of the evolution of the Tibetan Plateau according to the tectonic and thermal model of Hyndman (2019) is required. The geophysical studies of Xiao et al. (2020) indicate significant underthrusting of the Indian lower crust coupled with destruction of the Asian lithosphere under the western parts of the Tibet Plateau together with the presence of a steep down-dipping slab of Indian lithosphere. In Hyndman's (2019) model, the presence of a pre-collision hot back-arc is considered to weaken the lithosphere and is considered as a pre-collision requirement for orogenic deformation and crustal thickening rather than a consequence of orogeny. How these concepts will affect pre-exiting metasomes is not as yet understood.

Indian Lamproites

Apart from the complexities of their tectonic setting, studies of the petrogenesis of Indian lamproites have been hindered by problems in terminology resulting from resistance to using modern mineralogical-genetic classification schemes and undue reliance upon bulk rock geochemical studies. Many rocks previously described as "kimberlites" have now been reclassified as *bona fide* lamproites (Fareeduddin and Mitchell 2012; Gurmeet Kaur and Mitchell 2016). The numerous occurrences of "para-kimberlites" have not been investigated using detailed mineralogical studies and are probably varieties of olivine lamproite, e.g. the Tokapal epiclastic/pyroclastic vent which is typical of a lamproite volcano and not a kimberlite diatreme (Fareeduddin and Mitchell 2012). It is possible that archetypal kimberlites are absent from eastern and central India. Figure 20 shows that the known lamproites are emplaced in four Archean cratons, isolated from each other by Proterozoic mobile belts and rifts, which differ in geology, age, and genesis. A notable aspect of the distribution of most of the para-kimberlite and lamproite fields is that they form a SW–NE trending zone parallel to a zone of deformed undersaturated alkaline complexes emplaced within the Proterozoic polyphase granulite terrane of the Eastern Ghats Mobile Belt (Burke and Khan 2006). Exceptions are the Bunder and Majhgawan lamproites which are emplaced at the southern margins of the Bundelkhand craton adjacent to a different Proterozoic mobile belt. Lamproites are notably absent, or have not yet been discovered, from the Western Dharwar and Aravalli cratons. In the Eastern Dharwar craton, several lamproite provinces range in age from ~ 1350 Ma (Chelima) to ~ 1090 Ma (Wajrakurur) with most of the activity occurring at about 1.1 Ga. In the Bastar craton lamproites range in age from ~616 Ma (Tokapal) to 62–65 Ma (Kodomali, Bahradih). In the Singhbhum Craton lamproites were intruded into the Gondwana supracrustal sediments of the Damodar Valley Basins at
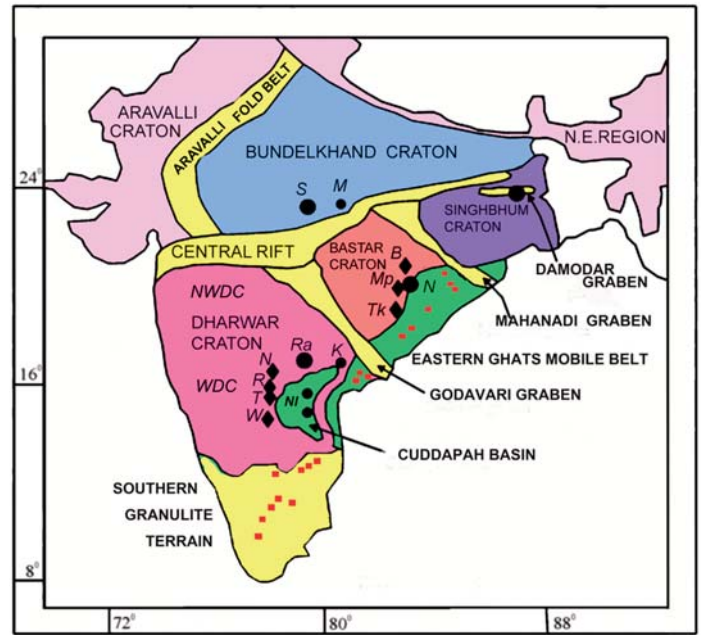

Figure 20. Distribution of lamproites (black circles: S - Saptarshi; M - Majhgawan; D - Damodar; Na - Nawapara; Ra - Ramadugu; K - Krishna; NI - Nallamalai-Chelima;), and lamproite-"para-kimberlite" fields (black labelled diamonds: B - Basna; Mp - Mainpur; Tk - Tokopal; N - Narayanpet; R - Raichur; T - Tungabhadra; W - Wajrakarur) in the cratons of the Indian subcontinent together with the locations of deformed Proterozoic alkaline rocks and carbonatites (red squares) in the Eastern Ghats Mobile Belt and Southern Granulite Terrain (after Gurmeet Kaur et al. 2018). Note that much of the northwestern part of the Dharwar craton (*NWDC*) is covered by Deccan Trap basalts which might account for the apparent absence of lamproites in that region but not the area (*WDC*) due west of the Narayanpet-Wajrakurur belt of lamproites of the Eastern Dharwar craton. Their absence might be related to the Archaean-Proterozoic paleo-subduction and origins of the Eastern Ghats Mobile Belt and formation of metasomes only within the eastern parts of the craton.

117–110 Ma and thus are of the same age as many of the Kaapvaal lamproites.

Each of the Indian lamproite provinces differs in mineralogy and age. Within each province there are typically several subfields consisting of para-kimberlites and lamproites of differing mineralogy, e.g. the Bokaro, Jharia, and Raniganj subfields of the Damodar Province, or the hypabyssal Wajrakurur Province which consists of the Wajrakurur, Lattavaram, Timmasamudram, and Chigicherla subfields. This observation implies that magmatism involves slightly different vein or wall-rock melting regimes within and between provinces, in some instances producing olivine lamproites, e.g. Lattavaram Pipe 3, or in others, more silica-rich lamproites, e.g. Wajrakurur P2-west (Fareeduddin and Mitchell 2012; Gurmeet Kaur and Mitchell 2013). In some provinces, differentiation of olivine phlogopite lamproite to leucite -K-feldspar lamproite is evident, e.g. Raniganj Province (Mukherjee 1961; Mitchell and Fareedduddin 2009). Shaikh et al. (2019) have concluded from an investigation of the trace element compositions of olivine in Wajrakurur (dykes CC2 and P13) and the Kodomali-Behradih lamproites that a hotter paleogeotherm existed in the lithospheric mantle beneath the Eastern Dharwar craton at ~ 1100 Ma than beneath the Bastar craton at ~ 65 Ma. In addition, it is proposed that the Eastern Dharwar craton experi-

enced a greater degree of metasomatism relative to the Bastar craton.

The initiation of partial melting of the metasomatized sources, which have been proposed for the diverse Indian lamproites, ranges from peripheral thermal effects of mantle plumes to regional asthenospheric upwelling and/or combinations of these processes. It is notable that the lamproites of the Eastern Dharwar craton have the same age as the Bunder-Majhgawan lamproites. However, as these lamproites are separated by 600 km, it is considered that hot spot magmatism could not have been involved in their simultaneous genesis (Helmstaedt 2018). In contrast, Kent et al. (1998) have concluded that Damodar magmatism was induced by partial melting at the margins of the Kerguelen hot spot, and it is suggested by Lehman et al. (2010) that the Kodomali and Behradih lamproites resulted from the plume that produced the Deccan traps. Note that a similar hypothesis has been advanced by Xiang et al. (2020) for the 260 Ma Baifen cratonic lamproites of the Yangtze Block (China) involving melting at the margins of the mantle plume initiating the Emeishan large igneous province. The common factor in these plume models is the rapid extension, thinning, and decompressional melting of the lithosphere induced by plume-related asthenospheric upwelling. However, as noted above with respect to the Leucite Hills other processes might be responsible for partial melting and these might be associated with a second period of incompatible enrichment of the ancient mantle metasomes.

Burke and Khan (2006) and Gurmeet Kaur et al. (2018) have interpreted the near-linear distribution of lamproites and alkaline rocks in eastern India parallel to the Eastern Ghats Mobile Belt (Fig. 20) to imply a relationship with ancient subduction processes on the basis of geophysical evidence for the presence of relict subducted oceanic slab material at depths of 160–220 km. This subducted slab is considered to be a product of the suturing of the Eastern Dharwar craton with the Eastern Ghats Mobile Belt at ~ 1600 Ma. Such subducted material might have been the source of metasomatic enrichment of the lithospheric mantle of the Dharwar and Baster cratons, but not the Singhbhum and Bundelkhand cratons. Localized partial melting of this source at ~ 1.1 Ga by asthenospheric upwelling could have resulted in the formation of the Dharwar lamproites, but not the younger Bastar lamproites or the Bundelkhand lamproites, implying different melting regimes for these magmas.

In common with the Kaapvaal craton, there has been erosion of the roots of the Dharwar and Bastar cratons. The lithospheric "keel" of the Bastar craton is estimated to have been at least 140 km in thickness at the time of emplacement of the Kodomali and Behradih lamproites, but is now only about 80–100 km in thickness, implying about one third of the craton root has been lost during the breakup of Gondwana (Lehman et al. 2010). The Eastern and Western Dharwar cratons have experienced similar modification with asthenospheric mantle now also being present at 80–100 km depth. Thus, the depleted lithospheric roots present 1.1 b.y. ago do not exist today (Griffin et al. 2009). Thermal erosion and delamination of these craton roots was considered by Lehman et al. (2010)

to be due to the eastern lateral deflection of the plume which produced the 68–65 Ma Deccan Traps toward the thinner lithosphere of eastern India.

The recent geophysical studies of the Kaapvaal and Indian cratons are instructive as they indicate that the ancient metasomatic sources of lamproites are no longer present, having been removed by younger tectonic events. Hence, the depths and temperatures of lamproite magma generation in the lithospheric mantle that have been estimated by the geothermobarometry of entrained eclogite and ultrabasic xenoliths refer to the paleo-configuration of the craton and not its current state (Shaikh et al. 2019). These observations, and the work of Celli et al. (2020), have implications for the genesis and preservation of lithospheric metasomes and highlight the need for detailed studies of the current and past structure of cratons. Many of the existing models for incorporation of diamond xenocrysts in lamproites and kimberlites (e.g. Haggerty 1989; Mitchell 1995a) are now considered too simplified, as they consider cratons to have a simple boat-like shape with a relatively uniform keel-shaped lithosphere–asthenosphere boundary. The paucity of lamproite magmatism in many cratons might be related to destruction of lithospheric metasomes during the generation and ascent of more voluminous asthenosphere-derived magmas such as the basalt of large igneous provinces.

FINAL COMMENTS AND FUTURE RESEARCH

Regardless of their rarity, lamproites remain of continuing petrological interest as they are a major source of diamonds and are magma types whose origins provide unique insights into metasomatic processes in the lithospheric mantle. Lamproite magmas have similar rheological characteristics to basaltic magmas and their emplacement as hypabyssal dykes and sills or phreatomagmatic vents is well characterized, although specific fields require further investigation, as shown by the recent re-investigation of the Cancarix volcano (Spain) by Reolid et al. (2015). The mineralogy and bulk-rock geochemistry of cratonic varieties is relatively well characterized. In contrast, although the trace element and isotope bulk-rock geochemistry of orogenic lamproites is well understood, especially as a result of recent studies of Tibetan occurrences, the details of the mineralogy of the minor and trace accessory minerals are less well characterized. The origins of lamproite magmas and the tectonic events that initiated their genesis remain ambiguous as individual lamproite provinces are unique with respect both to the mineralogy and geochemistry of their mantle sources and to the thermal events which initiate partial melting. Hence, the origins of a given lamproite must be evaluated on its own basis especially with regard to orogenic lamproites whose genesis involves recent subduction and mixing processes with mantle metasomes. Some aspects of lamproite petrology that require further investigation are:

1) detailed mineralogical and petrological investigations of the Majhgawan vent and para-kimberlites of the Dharwar and Bastar cratons of India.

2) characterization of lamproites and para-lamproites in the Aldan Shield (Russia), the São Francisco craton

(Brazil) and other South American localities (e.g. eastern Paraguay, Presser 2000), the southern West African craton (Bobi, Seguela), the Kapamba lamproites of the Luangwa graben (Zambia), and the west Greenland lamproites. The potassic rocks of the Aldan Shield in particular require much re-investigation because of the presence of extremely undersaturated ultrapotassic rocks (synnyrite, yakutite, etc.) in geographic, but not necessarily genetic, relationships with lamproite- and kamafugitic-like rocks (Kostyuk et al. 1990; Chayka et al. 2020).

3) explanations are required for the apparent paucity of cratonic lamproites in some cratons (Slave, Rae, Superior, Tanzanian, Yilgarn, Amazon), and of orogenic lamproites in the South America Cordillera. High resolution studies of the structure of cratons, their delamination and erosion following the methods of Celli et al. (2020) are essential.

4) modern methods of *in situ* analytical geochemistry, such as LA–ICP–MS, should be applied to individual minerals and glasses in lamproites to determine how particular elements are distributed for general petrogenetic purposes. Examples might include Rb, Cs, Pb, NH_4, and Tl abundances in phlogopite and the role of magma mixing; Sr, C, and O isotopic studies of the origins of carbonate in Kaapvaal lamproites; determination of the abundances of Pb and the Pb isotopic compositions of K-feldspar, and how Pb is sequestered in orogenic lamproites.

ACKNOWLEDGEMENTS

REFERENCES

Becker, M., and le Roex, A.P., 2006, Geochemistry of South African on- and off-craton, Group I and Group II kimberlites: petrogenesis and source region evolution: Journal of Petrology, v. 47, p. 673–703, https://doi.org/10.1093/petrology/egi089.

Boxer, G.L., Lorenz, V., and Smith, C.B., 1989, The geology and volcanology of the Argyle (AK1) lamproite diatreme, Western Australia: Geological Society of Australia, Special Publication 14, v. 1, p. 140–152.

Burke, K., and Khan, S., 2006, Geoinformatic approach to global nepheline syenite and carbonatite distribution: testing a Wilson cycle model: Geosphere, v. 2, p. 53–60, https://doi.org/10.1130/GES00027.1.

Carmichael, I.S.E., 1967, The mineralogy and petrology of the volcanic rocks from the Leucite Hills, Wyoming: Contributions to Mineralogy and Petrology, v. 15, p. 24–66, https://doi.org/10.1007/BF01167214.

Celli, N.L., Lebedev, S., Schaeffer, A.J., and Gaina, C., 2020, African cratonic lithosphere carved by mantle plumes: Nature Communications, v. 11, 92, https://doi.org/10.1038/s41467-019-13871-2.

Chalapathi Rao, N.V., 2005, A petrological and geochemical reappraisal of the Mesoproterozoic diamondiferous Majhgawan pipe of central India: evidence for a

transitional kimberlite – orangeite (group II kimberlite) – lamproite rock type: Mineralogy and Petrology, v. 84, p. 69–106, https://doi.org/10.1007/s00710-004-0072-2.

Chayka, I.F., Sobolev, A.V., Izokh, A.E., Batanova, V.G., Krasheninnikov, S.P., Chervyakovskaya, M.V., Kontonikas-Charos, A., Kutyrev, A.V., Lobastov, B.M., and Chervyakovskiy, V.S., 2020, Fingerprints of kamafugite-like magmas in Mesozoic lamproites of the Aldan Shield: Evidence from olivine and olivine-hosted inclusions: Minerals, v. 10, 337, https://doi.org/10.3390/min10040337.

Chen, J.-L., Xu, J.-F., Wang, B.-D., and Kang, Z.-Q., 2012, Cenozoic Mg-rich potassic rocks in the Tibetan Plateau: Geochemical variations, heterogeneity of subcontinental lithospheric mantle and tectonic implications: Journal of Asian Earth Sciences, v. 53, p. 115–130, https://doi.org/10.1016/j.jseaes.2012.03.003.

Clement, C.R., 1982, A comparative study of some major kimberlite pipes in the Northern Cape and Orange Free State: Unpublished Ph.D. thesis (2 volumes), University of Cape Town, South Africa, 432 p.

Coe, N., le Roex, A., Gurney, J., Pearson, D.G., and Nowell, G., 2008, Petrogenesis of the Swartruggens and Star Group II kimberlite dyke swarms, South Africa: constraints from whole rock geochemistry: Contributions to Mineralogy and Petrology, v. 156, 627, https://doi.org/10.1007/s00410-008-0305-01.

Conticelli, S., and Peccerillo, A., 1992, Petrology and geochemistry of potassic and ultrapotassic volcanism in central Italy: petrogenesis and inferences on the evolution of the mantle sources: Lithos, v. 28, p. 221–240, https://doi.org/10.1016/0024-4937(92)90008-M.

Conticelli, S., Manetti, P., and Menichetti, S., 1992, Mineralogy, geochemistry and Sr-isotopes in orendites from South Tuscany, Italy: constraints on their genesis and evolution: European Journal of Mineralogy, v. 4, p. 1359–1375.

Conticelli, S., D'Antonio, M., Pinarelli, L., and Civetta, L., 2002, Source contamination and mantle heterogeneity in the genesis of Italian potassic and ultrapotassic volcanic rocks: Sr–Nd–Pb isotope data from Roman Province and southern Tuscany: Mineralogy and Petrology, v. 74, p. 189–222, https://doi.org/10.1007/s007100200004.

Contini, S., Venturelli, G., Toscani, L., Capredi, S., and Barbieri, M., 1993, Cr–Zr-armalcolite-bearing lamproites of Cancarix, SE Spain: Mineralogical Magazine, v. 57, p. 203–216, https://doi.org/10.1180/minmag.1993.057.387.02.

Crawford, A.J., Falloon, T.J., and Green, D.H., 1989, Classification, petrogenesis and tectonic setting of boninites, in Crawford, A.J., ed., Boninites and Related Rocks: Unwin-Hyman, London, p. 1–49.

Cross, C.W., 1897, Igneous rocks of the Leucite Hills and Pilot Butte, Wyoming: American Journal of Science, v. 4, p. 115–141, https://doi.org/10.2475/ajs.s4-4.20.115.

Das, H., Kobussen, A.F., Webb, K.J., Phillips, D., Maas, R., Soltys, A., Rayner, M.J., and Howell, D., 2018, The Bunder Diamond project, India: Geology, geochemistry and age of the Saptarshi lamproite pipes, in Davy, A.T., Smith, C.B., Helmstaedt, H., Jaques, A.L., and Gurney, J.J., eds., Geoscience and Exploration of the Argyle, Bunder, Diavik, and Murowa Diamond Deposits: Society of Economic Geologists Special Publication, v. 20, p. 201–222, https://doi.org/10.5382/SP.20.09.

Dawson, J.B., 1987, The kimberlite clan: relationship with olivine and leucite lamproites, and inferences for upper-mantle metasomatism, in Fitton, J.G., and Upton, B.G.J., eds., Alkaline Igneous Rocks: Geological Society, London, Special Publications, v. 30, p. 95–101, https://doi.org/10.1144/GSL.SP.1987.030.01.07.

Dawson, J.B., and Smith, J.V., 1977, The MARID (mica-amphibole-rutile-ilmenite-diopside) suite of xenoliths in kimberlite: Geochimica et Cosmochimica Acta, v. 41, p. 309–310, IN9-IN11, 311–323, https://doi.org/10.1016/0016-7037(77)90239-3.

Dunn, D.P., 2002, Xenolith mineralogy and geology of the Prairie Creek lamproite province, Arkansas: Unpublished Ph.D. thesis, University of Texas at Austin, 147 p., hdl.handle.net/2152/554.

Ekkerd, J., Stiefenhofer, J., Field, M., and Lawless, P., 2006, The geology of Finsch Mine, northern Cape Province, South Africa: 8th International Kimberlite Conference, Kimberlite Emplacement Workshop, Saskatoon, Canada, Extended Abstracts, FLA_0310, https://doi.org/10.29173/ikc3204.

Fareeduddin, and Mitchell, R.H., 2012, Diamonds and their source rocks in India: Geological Society of India, Bangalore, 434 p.

Field, M., Stiefenhofer, J., Robey, J., and Kurszlaukis, S., 2008, Kimberlite-hosted diamond deposits of southern Africa: A review: Ore Geology Reviews, v. 34, p. 33–75, https://doi.org/10.1016/j.oregeorev.2007.11.002.

Foley, S., 1992a, Petrological characterization of the source components of potassic magmas: Geochemical and experimental constraints: Lithos, v. 28, p. 187–204, https://doi.org/10.1016/0024-4937(92)90006-K.

Foley, S., 1992b, Vein-plus-wall-rock melting mechanisms in the lithosphere and the origin of potassic alkaline magmas: Lithos, v. 28, p. 435–453,

https://doi.org/10.1016/0024-4937(92)90018-T.

Foley, S.F., Venturelli, G., Green, D.H., and Toscani, L., 1987, The ultrapotassic rocks: characteristics, classification and constraints for petrogenetic models: Earth-Science Reviews, v. 24, p. 81–134, https://doi.org/10.1016/0012-8252(87)90001-8.

Franklin, J., 1822, On the diamond mines of Panna in Bundelkhand: Asia Research, v. 18, p. 100–122.

Gaeta, M., Freda, C., Marra, F., Di Rocco, T., Gozzi, F., Arienzo, I., Giaccio, B., and Scarlato, P., 2011, Petrology of the most recent ultrapotassic magmas of the Roman Province (Central Italy): Lithos, v. 127, p. 298–308, https://doi.org/10.1016/j.lithos.2011.08.006.

Gao, Y., Hou, Z., Kamber, B.S., Wei, R., Meng, X., and Zhao, R., 2007, Lamproitic rocks from a continental collision zone: Evidence for recycling of subducted Tethyan oceanic sediments in the mantle beneath southern Tibet: Journal of Petrology, v. 48, p. 729–752, https://doi.org/10.1093/petrology/egl080.

Ge, C., Sun, Y., Toksöz, M.N., Zheng, Y., Zheng, Y., Xiong, X., and Yu, D., 2012, Crustal structure of the central Tibetan plateau and geological interpretation: Earthquake Science, v. 25, p. 363–370, https://doi.org/10.1007/s11589-012-0862-2.

Giuliani, A., Phillips, D., Woodhead, J.D., Kamenetsky, V.S., Fiorentini, M.L., Mass, R., Soltys, A., and Armstrong, R.A., 2015, Did diamond-bearing orangeites originate from MARID-veined peridotites in the lithospheric mantle?: Nature Communications, v. 6, 6837, https://doi.org/10.1038/ncomms7837.

Griffin, W.L., Kobussen, A.F., Babu, E.V.S.S.K., O'Reilly, S.Y., Norris, R., and Sengupta, P., 2009, A translithospheric suture in the vanished 1-Ga lithospheric root of South India: Evidence from contrasting lithosphere sections in the Dharwar Craton: Lithos, v. 112, p. 1109–1119, https://doi.org/10.1016/j.lithos.2009.05.015.

Guo, Z., Wilson, M., Zhang, M., Cheng, Z., and Zhang, L., 2015, Post-collisional ultrapotassic mafic magmatism in south Tibet: Products of partial melting of pyroxenite in the mantle wedge induced by roll-back and delamination of the subducted Indian continental lithosphere slab: Journal of Petrology, v. 56, p. 1365–1406, https://doi.org/10.1093/petrology/egv040.

Gurmeet Kaur, and Mitchell, R.H., 2013, Mineralogy of the P2-West 'kimberlite', Wajrakarur kimberlite field, Andhra Pradesh, India: kimberlite or lamproite?: Mineralogical Magazine, v. 77, p. 3175–3196, https://doi.org/10.1180/minmag.2013.077.8.11.

Gurmeet Kaur, and Mitchell, R.H., 2016, Mineralogy of the P-12 K-Ti-richterite diopside olivine lamproite from Wajrakarur, Andhra Pradesh, India: implications for subduction-related magmatism in eastern India: Mineralogy and Petrology, v. 110, p. 223–245, https://doi.org/10.1007/s00710-015-0402-6.

Gurmeet Kaur, Mitchell, R.H., and Ahmed, S., 2018, Mineralogy of the Vattikod lamproite dykes, Ramadugu lamproite field, Nalgonda District, Telangana: A possible expression of ancient subduction-related alkaline magmatism along Eastern Ghats Mobile Belt, India: Mineralogical Magazine, v. 82, p. 35–58, https://doi.org/10.1180/minmag.2017.081.045.

Haggerty, S.E., 1989, Mantle metasomes and the kinship between carbonatite and kimberlites, in Bell, K., ed., Carbonatites: Unwin Hyman, London, p. 546–560.

Haggerty, S.E., 1995, Upper mantle mineralogy: Journal of Geodynamics, v. 20, p. 331–364, https://doi.org/10.1016/0264-3707(95)00016-3.

Helmstaedt, H., 2018, Tectonic and structural controls on diamondiferous kimberlite and lamproite and their bearing on area selection for diamond exploration, in Davy, A.T., Smith, C.B., Helmstaedt, H., Jaques, A.L., and Gurney, J.J., eds., Geoscience and Exploration of the Argyle, Bunder, Diavik, and Murowa Diamond Deposits: Society of Economic Geologists, Special Publication, v. 20, p. 1–48.

Hernández-Uribe, D., and Palin, R.M., 2019, Catastrophic shear-removal of subcontinental lithospheric mantle beneath the Colorado Plateau by the subducted Farallon slab: Nature Scientific Reports, v. 9, 8153, https://doi.org/10.1038/s41598-019-44628-y.

Hickey, R.L., and Frey, F.A., 1982, Geochemical characteristics of boninite series volcanics: Implications for their source: Geochimica et Cosmochimica Acta, v. 46, p. 2099–2115, https://doi.org/10.1016/0016-7037(82)90188-0.

Hyndman, R.D., 2019, Mountain building orogeny in pre-collision hot backarcs: North American Cordillera, India-Tibet, and Grenville Province: Journal of Geophysical Research, v. 124, p. 2057–2079, https://doi.org/10.1029/2018JB016697.

Jaques, A.L., Lewis, J.D., and Smith, C.B., 1986, The kimberlites and lamproites of Western Australia: Geological Survey of Western Australia, Bulletin 132, 268 p.

Jaques, A.L., Brink, F., and Chen, J., in press, Magmatic haggertyite in olivine lamproites of the West Kimberley region, Western Australia: American Mineralogist, https://doi.org/10.2138/am-2020-7456.

Kent, R.W., Kelley, S.P., and Pringle, M.S., 1998, Mineralogy and $^{40}Ar/^{39}Ar$

geochronology of orangeites (Group II kimberlites) from the Damodar Valley, eastern India: Mineralogical Magazine, v. 62, p. 313–323, https://doi.org/10.1180/002646198547701.

Kostyuk, V.P., Panina, L.L., Zhidkov, A.Y., Orlova, M.P., and Bazarova, T.Y., 1990, Potassic alkaline magmatism of the Baikal-Stanovoy Rifting System: Nauka, Novosibirsk, 200 p. (in Russian).

Krmíček, L., Cempírek, J., Havlín, A., Přichystal, A., Houzar, S., Krmíčková, M., and Gadas, P., 2011, Mineralogy and petrogenesis of a Ba–Ti–Zr-rich peralkaline dyke from Šebkovice (Czech Republic): Recognition of the most lamproitic Variscan intrusion: Lithos, v. 121, p. 74–86, https://doi.org/10.1016/j.lithos.2010.10.005.

Krmíček, L., Romer, R.L., Ulrych, J., Glodny, J., and Prelević, D., 2016, Petrogenesis of orogenic lamproites of the Bohemian Massif: Sr–Nd–Pb–Li isotope constraints for Variscan enrichment of ultra-depleted mantle domains: Gondwana Research, v. 35, p. 198–216, https://doi.org/10.1016/j.gr.2015.04.012.

Lange, R.A., Carmichael, I.S.E., and Hall, C.M., 2000, $^{40}Ar/^{39}Ar$ chronology of the Leucite Hills, Wyoming: Eruption rates, erosion rates, and an evolving temperature structure of the underlying mantle: Earth and Planetary Science Letters, v. 174, p. 329–340, https://doi.org/10.1016/S0012-821X(99)00267-8.

Lehmann, B., Burgess, R., Frei, D., Belyatsky, B., Mainkar, D., Chalapathi Rao, N.V., and Heaman, L.M., 2010, Diamondiferous kimberlites in central India synchronous with Deccan flood basalts: Earth and Planetary Sciences Letters, v. 290, p. 142–149, https://doi.org/10.1016/j.epsl.2009.12.014.

Levander, A., Schmandt, B., Miller, M.S., Liu, K., Karlstrom, K.E., Crow, R.S., Lee, C.-T.A., and Humphreys, E.D., 2011, Continuing Colorado plateau uplift by delamination-style convective lithospheric downwelling: Nature, v. 472, p. 461–465, https://doi.org/10.1038/nature10001.

Lustrino, M., Agostini, S., Chalal, Y., Fedele, L., Stagno, V., Colombi, F., and Bouguerra, A., 2016, Exotic lamproites or normal ultrapotassic rocks? The Late Miocene volcanic rocks from Kef Hahouner, NE Algeria, in the frame of the circum-Mediterranean lamproites: Journal of Volcanology and Geothermal Research, v. 327, p. 539–553, https://doi.org/10.1016/j.jvolgeores.2016.09.021.

Lustrino, M., Fedele, L., Agostini, S., Prelević, D., and Salari, G., 2019, Leucitites within and around the Mediterranean area: Lithos, v. 324–325, p. 216–233, https://doi.org/10.1016/j.lithos.2018.11.007.

Masun, K., Sthapak, A.V., Singh, A., Vaidya, A., and Krishna, C., 2009, Exploration history and geology of the diamondiferous ultramafic Saptarshi intrusions, Madhya Pradesh, India: Lithos, v. 112S, p. 142–154, https://doi.org/10.1016/j.lithos.2009.06.003.

Mathur, S.M., and Singh, H.N., 1971, Petrology of the Majhgawan pipe rocks: Geological Survey of India, Miscellaneous Publication, v. 19, p. 78–85.

McCulloch, M.T., Jaques, A.L., Nelson, D.R., and Lewis, J.D., 1983, Nd and Sr isotopes in kimberlites and lamproites from Western Australia: An enriched mantle origin: Nature, v. 302, p. 400–403, https://doi.org/10.1038/302400a0.

Meyer, H.O.A., 1976, Kimberlites of the continental United States: A Review: The Journal of Geology, v. 84, p. 377–403, https://dx.doi/10.2307/30066057.

Miller, C., Schuster, R., Klötzli, U., Frank, W., and Purtscheller, F., 1999, Post-collisional potassic and ultrapotassic magmatism in SW Tibet: Geochemical and Sr–Nd–Pb–O isotopic constraints for mantle source characteristics and petrogenesis: Journal of Petrology, v. 40, p. 1399–1424, https://doi.org/10.1093/petroj/40.9.1399.

Mirnejad, H., and Bell, K., 2006, Origin and source evolution of the Leucite Hills lamproites: evidence from Sr–Nd–Pb–O isotopic compositions: Journal of Petrology, v. 47, p. 2463–2489, https://doi.org/10.1093/petrology/egl051.

Mitchell, R.H., 1986, Kimberlites: Mineralogy, Geochemistry, and Petrology: Plenum Press, New York, 442 p.

Mitchell, R.H., 1995a, Kimberlites, Orangeites and Related Rocks: Plenum Press, New York, 410 p., https://doi.org/10.1007/978-1-4615-1993-5.

Mitchell, R.H., 1995b, Melting experiments on a sanidine phlogopite lamproite at 4–7 GPa and their bearing on the sources of lamproitic magmas: Journal of Petrology, v. 36, p. 1455–1474, https://doi.org/10.1093/petrology/36.5.1455.

Mitchell, R.H., 1996, Undersaturated potassic plutonic complexes, in Mitchell, R.H., ed., Undersaturated Alkaline Rocks: Mineralogy, Petrogenesis and Economic Potential: Mineralogical Association of Canada Short Course, v. 24, p. 193–216.

Mitchell, R.H., 1997, Kimberlites, Orangeites, Lamproites, Melilitites, and Minettes: A Petrographic Atlas: Almaz Press, Thunder Bay, Ontario, Canada, 234 p.

Mitchell, R.H., 2006, Potassic magmas derived from metasomatized lithospheric mantle: Nomenclature and relevance to exploration for diamond-bearing rocks: Journal of the Geological Society of India, v. 67, p. 317–327.

Mitchell, R.H., 2007, Potassic rocks from the Gondwana Coalfields of India: Closing Pandora's Box of petrological confusion?: Journal of the Geological Society of India, v. 69, p. 505–512.

Mitchell, R.H., and Bergman, S.C., 1991, Petrology of Lamproites: Plenum Press,

New York, 447 p., https://doi.org/10.1007/978-1-4615-3788-5.

Mitchell, R.H., and Fareeduddin, 2009, Mineralogy of peralkaline lamproites from the Raniganj Coalfield, India: Mineralogical Magazine, v. 73, p. 457–477, https://doi.org/10.1180/minmag.2009.073.3.457.

Mitchell, R.H., Platt, RG., and Downey, M., 1987, Petrology of lamproites from Smoky Butte, Montana: Journal of Petrology, v. 28, p. 645–677.

Mitchell, R.H., Giuliani, A., and O'Brien, H., 2019, What is a kimberlite? Petrology and mineralogy of hypabyssal kimberlites: Elements, v. 15, p. 381–386, https://doi.org/10.2138/gselements.15.6.381.

Mo, X., Zhao, Z., Deng, J., Flower, M., Yu, X., Luo, Z., Li, Y., Zhou, S., Dong, G., Zhu, D., and Wang, L., 2006, Petrology and geochemistry of postcollisional volcanic rocks from the Tibetan plateau: Implications for lithosphere heterogeneity and collision-induced asthenospheric mantle flow, *in* Dilek, Y., and Pavlides, S., *eds.*, Postcollisional Tectonics and Magmatism in the Mediterranean Region and Asia: Geological Society of America Special Papers, v. 409, p. 507–530, https://doi.org/10.1130/2006.2409(24).

Mukherjee, K.K., 1961, Petrology of the lamprophyres of the Bokaro coalfield: Quarterly Journal of the Mineralogical and Metallurgical Society of India, v. 33, p. 69–87.

Nelson, D.R., McCulloch, M.T., and Sun, S.-S., 1986, The origins of ultrapotassic rocks as inferred from Sr, Nd, and Pb isotopes: Geochimica et Cosmochimica Acta, v. 50, p. 231–245, https://doi.org/10.1016/0016-7037(86)90172-9.

Niggli, P., 1923, Gesteins und Mineralprovinzen: Verlag Gebrüder Borntraegar, Berlin, 586 p.

O`Brien, H.E., Irving, A.J., McCallum, I.S., and Thirwall, M.F., 1995, Strontium, neodymium, and lead isotopic evidence for the interaction of post-subduction asthenospheric potassic mafic magmas of the Highwood Mountains, Montana, USA, with ancient Wyoming craton lithospheric mantle: Geochimica et Cosmochimica Acta, v. 59, p. 4539–4556, https://doi.org/10.1016/0016-7037(95)99266-J.

Osann, A., 1906, Über einige Alkaligestein aus Spanien: Festschrift Rosenbusch, Stuttgart, p. 283–301.

Pearson, D.G., Woodhead, J., and Janney, P.E., 2019, Kimberlites as geochemical probes of the Earth's mantle: Elements, v. 15, p. 387–392, https://doi.org/10.2138/gselements.15.6.387.

Pe-Piper, G., Zhang, Y., Piper, D.J.W., and Prelević, D., 2014, Relationship of Mediterranean-type lamproites to large shoshonite volcanoes, Miocene of Lesbos, NE Aegean Sea: Lithos, v. 184–187, p. 281–299, https://doi.org/10.1016/j.lithos.2013.11.004.

Prelević, D., and Foley, S.F., 2007, Accretion of arc-oceanic lithospheric mantle in the Mediterranean: Evidence from extremely high-Mg olivines and Cr-rich spinel inclusions in lamproites: Earth and Planetary Science Letters, v. 256, p. 120–135, https://doi.org/10.1016/j.epsl.2007.01.018.

Prelević, D., Foley, S.F., Romer, R.L., Cvetković, V., and Downes, H., 2005, Tertiary ultrapotassic volcanism in Serbia: constraints on petrogenesis and mantle source characteristics: Journal of Petrology, v. 46, p. 1443–1487, https://doi.org/10.1093/petrology/egi022.

Prelević, D., Akal, C., Foley, S.F., 2008a, Orogenic vs anorogenic lamproites in a single volcanic province: Mediterranean-type lamproites from Turkey: Don Harrington Symposium on the Geology of the Aegean, IOP Conference Series: Earth and Environmental Science 2; IOP Publishing, 012024, https://doi.org/10.1088/1755-1307/2/1/012024.

Prelević, D., Foley, S.F., Romer, R., and Conticelli, S., 2008b, Mediterranean Tertiary lamproites derived from multiple source components in postcollisional geodynamics: Geochimica et Cosmochimica Acta, v. 72, p. 2125–2156, https://doi.org/10.1016/j.gca.2008.01.029.

Prelević, D., Stracke, A., Foley, S.F., Romer, R.L., and Conticelli, S., 2010, Hf isotope compositions of Mediterranean lamproites: Mixing of melts from asthenosphere and crustally contaminated mantle lithosphere: Lithos, v. 119, p. 297–312, https://doi.org/10.1016/j.lithos.2010.07.007.

Presser, J.L.B., 2000, Lamproites of the Ybytyruzú field, Guairá Department, Eastern Paraguay (Abstract): International Brazil 2000, First International Geological Congress.

Rao, T.K., 2007, Panna Diamond Belt, Madhya Pradesh – A critical review: Journal of the Geological Society of India, v. 69, p. 513–522.

Rayner, M.J., Jaques, A.L., Boxer, G.L., Smith, C.B., Lorenz, V., Moss, S.W., Webb, K., and Ford, D., 2018, The geology of the Argyle (AK1) diamond deposit, Western Australia, *in* Davy, A.T., Smith, C.B., Helmstaedt, H., Jaques, A.L., and Gurney, J.J., *eds.*, Geoscience and Exploration of the Argyle, Bunder, Diavik, and Murowa Diamond Deposits: Society of Economic Geologists, Special Publication, v. 20, p. 89–117, https://doi.org/10.5382/SP.20.04.

Reolid, M., Abad, I., and Sanchez-Gomez, M., 2015, Phreatomagmatic activity and associated hydrothermal processes in the lamproitic volcano of Cancarix (Southeast Spain): Journal of Iberian Geology, v. 41, p. 183–204, https://doi.org/10.5209/rev_JIGE.2015.v41.n2.46696.

Roffey, S., Rayner, M.J., Davy, A.T., and Platell, R.W., 2018, Evaluation of the AK1 Deposit at Argyle Diamond Mine, *in* Davy, A.T., Smith, C.B., Helmstaedt, H., Jaques, A.L., and Gurney, J.J., *eds.*, Geoscience and Exploration of the Argyle, Bunder, Diavik, and Murowa Diamond Deposits: Society of Economic Geologists, Special Publication, v. 20, p. 65–87, https://doi.org/10.5382/SP.20.03.

Scott Smith, B.H., 1989, Lamproites and kimberlites in India: Neues Jahrbuch für Mineralogie Abhandlungen, v. 161, p. 193–225.

Scott Smith, B.H., 2008, The Fort à la Corne kimberlites, Saskatchewan, Canada: Geology, emplacement and economics: Journal of the Geological Society of India, v. 71, p. 11–55.

Scott Smith, B.H., and Skinner, E.M.W., 1984, Diamondiferous lamproites: Journal of Geology, v. 92, p. 433–438, https://doi.org/10.1086/628877.

Scott Smith, B.H., Nowicki, T.E., Russell, J.K., Webb, K.J., Mitchell, R.H., Hetman, C.M., and Robey, J.vA., 2018, A Glossary of Kimberlite and Related Terms Part 1: Scott-Smith Petrology Inc., North Vancouver, British Columbia, Canada, 144 p.

Shaikh, A.M., Patel, S.C., Bussweiler, Y., Kumar, S.P., Tappe, S., Ravi, S., and Mainkar, D., 2019, Olivine trace element compositions in diamondiferous lamproites from India: Proxies for magma origins and the nature of the lithospheric mantle beneath the Bastar and Dharwar cratons: Lithos, v. 324–325, p. 501–518, https://doi.org/10.1016/j.lithos.2018.11.026.

Shand, S.J., 1922, The problem of the alkaline rocks: Proceedings of the Geological Society of South Africa, v. 25, p. xix–xxxii.

Smith, C.B., 1983, Pb, Sr and Nd isotopic evidence for sources of southern African Cretaceous kimberlites: Nature, v. 304, p. 51–54, https://doi.org/10.1038/304051a0.

Smith, C.B., Skinner, E.M.W., Clement, C.R., Gurney, J.J., and Ebrahim, N., 1985, Geochemical character of southern African kimberlites: A new approach based on isotopic constraints: Transactions of the Geological Society of South Africa, v. 88, p. 267–280.

Venturelli, G., Capedri, S., Di Battistini, G., Crawford, A., Kogarko, L.N., and Celestini, S., 1984, The ultrapotassic rocks from southeastern Spain: Lithos, v. 17, p. 37–54, https://doi.org/10.1016/0024-4937(84)90005-7.

Vollmer, R., Ogden, P., Schilling, J.-G., Kingsley, R.H., and Waggoner, D.G., 1984, Nd and Sr isotopes in ultrapotassic volcanic rocks from the Leucite Hills, Wyoming: Contributions to Mineralogy and Petrology, v. 87, p. 359–368, https://doi.org/10.1007/BF00381292.

Wade, A., and Prider, R.T., 1940, The leucite-bearing rocks of the West Kimberley area, Western Australia: Quarterly Journal of the Geological Society, v. 96, p. 39–98, https://doi.org/10.1144/GSL.JGS.1940.096.01-04.04.

Wagner, P.A., 1914, The Diamond Fields of Southern Africa: Transvaal Leader, Johannesburg, 355 p.

Wagner, P.A., 1928, The evidence of the kimberlite pipes on the constitution of the outer part of the Earth: South African Journal of Science, v. 25, p. 127–148.

Woolley, A.R., Bergman, S.C., Edgar, A.D., Le Bas, M.J., Mitchell, R.H., Rock, N.M.S., and Scott Smith, B.H., 1996, Classification of lamprophyres, lamproites, kimberlites, and the kalsilitic, melilitic, and leucitic rocks: Canadian Mineralogist, v. 34, p. 175–186.

Xia, L., Li, X., Ma, Z., Xu, X., and Xia, Z., 2011, Cenozoic volcanism and tectonic evolution of the Tibetan plateau: Gondwana Research, v. 19, p. 850–866, https://doi.org/10.1016/j.gr.2010.09.005.

Xiang, L., Zheng, J., Zhai, M., and Siebel, W., 2020, Geochemical and Sr–Nd–Pb isotopic constraints on the origin and petrogenesis of Paleozoic lamproites in the southern Yangtze Block, South China: Contributions to Mineralogy and Petrology, v. 175, 29, https://doi.org/10.1007/s00410-020-1668-1.

Xiao, Z., Fuji, N., Iidaka, T., Gao, Y., Sun, X., and Liu, Q., 2020, Seismic structure beneath the Tibetan Plateau from iterative finite-frequency tomography based on ChinArray: New insights into the Indo-Asian collision: Journal of Geophysical Research, v. 125, e2019JB018344, https://doi.org/10.1029/2019JB018344.

Zhang, L., Guo, Z., Zhang, M., Cheng, Z., and Sun, Y., 2017, Post-collisional potassic magmatism in the eastern Lhasa terrane, South Tibet: Products of partial melting of mélanges in a continental subduction channel: Gondwana Research, v. 41, p. 9–28, https://doi.org/10.1016/j.gr.2015.11.007.